

2022

## Contrasting controls on seasonal and spatial distribution of marine cable bacteria (*Candidatus Electrothrix*) and *Beggiatoaceae* in seasonally hypoxic Chesapeake Bay

Sairah Y. Malkin

Pinky Liao

Carol Kim

Kalev G. Hantsoo

Maya L. Gomes

*See next page for additional authors*

Follow this and additional works at: <https://scholarworks.wm.edu/vimsarticles>



Part of the [Marine Biology Commons](#)

---

### Recommended Citation

Malkin, Sairah Y.; Liao, Pinky; Kim, Carol; Hantsoo, Kalev G.; Gomes, Maya L.; and Song, Bongkeun, Contrasting controls on seasonal and spatial distribution of marine cable bacteria (*Candidatus Electrothrix*) and *Beggiatoaceae* in seasonally hypoxic Chesapeake Bay (2022). *Limnology and Oceanography*.

doi: 10.1002/lno.12087

This Article is brought to you for free and open access by the Virginia Institute of Marine Science at W&M ScholarWorks. It has been accepted for inclusion in VIMS Articles by an authorized administrator of W&M ScholarWorks. For more information, please contact [scholarworks@wm.edu](mailto:scholarworks@wm.edu).

---

**Authors**

Sairah Y. Malkin, Pinky Liao, Carol Kim, Kalev G. Hantsoo, Maya L. Gomes, and Bongkeun Song

# Contrasting controls on seasonal and spatial distribution of marine cable bacteria (*Candidatus Electrothrix*) and Beggiatoaceae in seasonally hypoxic Chesapeake Bay

Sairah Y. Malkin <sup>1\*</sup>, Pinky Liao,<sup>1</sup> Carol Kim,<sup>1</sup> Kaley G. Hantsoo <sup>2</sup>, Maya L. Gomes <sup>2</sup>, Bongkeun Song <sup>3</sup>

<sup>1</sup>Horn Point Laboratory, University of Maryland Center for Environmental Science (UMCES), Cambridge, Maryland

<sup>2</sup>Department of Earth and Planetary Sciences, Johns Hopkins University, Baltimore, Maryland

<sup>3</sup>Virginia Institute of Marine Science, College of William and Mary, Gloucester Point, Virginia

## Abstract

Marine cable bacteria (*Candidatus Electrothrix*) and large colorless sulfur-oxidizing bacteria (e.g., Beggiatoaceae) are widespread thiotrophs in coastal environments but may exert different influences on biogeochemical cycling. Yet, the factors governing their niche partitioning remain poorly understood. To map their distribution and evaluate their growth constraints in a natural setting, we examined surface sediments across seasons at two sites with contrasting levels of seasonal oxygen depletion in Chesapeake Bay using microscopy coupled with 16S rRNA gene amplicon sequencing and biogeochemical characterization. We found that cable bacteria, dominated by a single phylotype closely affiliated to *Candidatus Electrothrix* communis, flourished during winter and spring at a central channel site which experiences summer anoxia. Here, cable bacteria density was positively correlated with surface sediment chlorophyll, a proxy of phytodetritus sedimentation. Cable bacteria were also present with a lower areal density at an adjacent shoal site which supports bioturbating macrofauna. Beggiatoaceae were more abundant at this site, where their biomass was positively correlated with sediment respiration, but additionally potentially inhibited by sulfide accumulation which was evident during one summer. A springtime phytodetritus sedimentation event was associated with a proliferation of Beggiatoaceae and multiple *Candidatus Electrothrix* phylotypes, with cable bacteria reaching 1000 m length  $\text{cm}^{-2}$ . These observations indicate the potential impact of a spring bloom in driving a hot moment of cryptic sulfur cycling. Our results suggest complex interactions between benthic thiotroph populations, with bioturbation and seasonal oscillations in bottom water dissolved oxygen, sediment sulfide, and organic matter influx as important drivers of their distribution.

A widespread feature of surficial coastal sediments overlain by an oxygenated water column is the presence of a suboxic zone, defined as a sediment space where both oxygen and sulfide are absent, despite potentially high rates of sulfide production by microbial sulfate reduction (Jørgensen et al. 2019).

This feature can be millimeters to centimeters wide and may function as an important barrier to sulfide diffusion from sediments (Seitaj et al. 2015). The accumulation of sulfide is commonly inhibited by the continuous replenishment of reactive metal oxides, fostered by the activities of bioturbating macrofauna (Kristensen 2000). Suboxic zones may also be maintained by the activities of “gradient microorganisms,” specialized microbes capable of oxidizing sulfide by coupling its oxidation with nitrate or oxygen across the suboxic space (Wasmund et al. 2017). In coastal sediments, at least two distinct microbial strategies have been reported as quantitatively important for sulfide removal over centimeter-scale distances.

One microbial strategy for oxidizing sulfide in sediments is carried out by the large colorless sulfur-oxidizing Gammaproteobacteria, such as Beggiatoaceae (Teske and Salman 2014). Members of the family Beggiatoaceae have been the subject of microbial bioenergetics studies since the formative chemoautotrophy investigations of Winogradsky in the

\*Correspondence: smalkin@umces.edu

This is an open access article under the terms of the Creative Commons Attribution-NonCommercial License, which permits use, distribution and reproduction in any medium, provided the original work is properly cited and is not used for commercial purposes.

Additional Supporting Information may be found in the online version of this article.

**Author Contribution Statement:** S.Y.M. conceived of the study and drafted the manuscript. S.Y.M., P.L., C.K., K.H., M.G., and B.S. contributed substantially to the data acquisition and analysis. All authors provided substantive input to the manuscript and approved the final submitted version.

late 19<sup>th</sup> century (Ackert 2013). These bacteria grow as large filaments with gliding motility and many are capable of transporting nitrate in vacuoles for use as an electron acceptor through suboxic sediments, reducing nitrate to ammonia (Mußmann et al. 2003, 2007). Some of these couple the oxidation of sulfur directly with oxygen (Schwedt et al. 2012). The sulfur oxidation activity of Beggiatoaceae imparts a distinct imprint on pore water pH, with a minimum near the oxic or nitrate horizons, and a pH maximum at the sulfide horizon (Sayama et al. 2005; Seitaj et al. 2015). Where their densities are high, Beggiatoaceae filaments may maintain and deepen a suboxic zone (Fenchel and Bernard 1995; Sayama et al. 2005).

Another distinct mechanism occurs by the electron-conducting cable bacteria (Malkin et al. 2015; Seitaj et al. 2015; Burdorf et al. 2016), which are affiliated to the family Desulfobulbaceae (Trojan et al. 2016). In contrast to Beggiatoaceae, sulfur oxidation by cable bacteria was only relatively recently discovered (Nielsen et al. 2010; Pfeiffer et al. 2012). These long filamentous bacteria span the suboxic zone and catalyze sulfide oxidation by commuting electrons along their longitudinal axis from sulfide-generating sediments to the oxic zone, connecting distances as great as ~3 cm (Schauer et al. 2014; Meysman et al. 2015; Bjerg et al. 2018). Among cable bacteria, the genus *Candidatus Electrothrix* dominates in marine sediments (Trojan et al. 2016; Dam et al. 2021). Cable bacteria have demonstrated rapid growth (Schauer et al. 2014), and accumulating evidence indicates these bacteria play an important and unique role in biogeochemical cycling in marine coastal systems (Risgaard-Petersen et al. 2012; Nielsen and Risgaard-Petersen 2015; Seitaj et al. 2015). Like Beggiatoaceae, cable bacteria are capable of reducing inorganic nitrogen sources to ammonia but not to dinitrogen gas (Risgaard-Petersen et al. 2014; Kjeldsen et al. 2019; Marzocchi et al. 2022). In addition, cable bacteria can dominate the biological oxygen demand in organic-rich sediments, removing free sulfide to several centimeters depth (Risgaard-Petersen et al. 2012; Nielsen and Risgaard-Petersen 2015; Rao et al. 2016). The anodic oxidation of cable bacteria generates acidity, creating a deep pH-minimum that leaves a distinct imprint of their activity in sediments (Nielsen et al. 2010; Meysman et al. 2015; Seitaj et al. 2015). This acidity causes dissolution of iron monosulfides (FeS) (Risgaard-Petersen et al. 2012; Larsen et al. 2014; Rao et al. 2016), which drives an accumulation of iron oxides near the sediment surface, delaying euxinic conditions from developing in bottom waters during seasonal anoxia (Seitaj et al. 2015). The consequent FeS dissolution also affects microbial activity, for example, stimulating dissimilatory nitrate reduction to ammonia (Kessler et al. 2019). The acid dissolution also alters carbonate burial efficiency (Rao et al. 2016) and has been associated with production of pore water manganese (II), retention of dissolved organic carbon, removal of pore water phosphate, resupply of sulfate (Sulu-Gambari et al. 2015, 2016; Sandfeld et al. 2020), and mobilization of the trace metals arsenic and

cobalt (van de Velde et al. 2017). In short, where abundant, cable bacteria may impart quantitatively important consequences for a multitude of biogeochemical processes near the sediment water interface.

In order to quantify the roles of marine Beggiatoaceae and cable bacteria in sediment ecology and ecosystem-level biogeochemical cycling, a better understanding is needed of their distribution, activity, and growth constraints. The main objective of this work was to track the seasonality of these sulfur-oxidizing bacteria in Chesapeake Bay, a semi-tropical seasonally oxygen-depleted estuarine system. We investigated a pair of study sites that both lie in the mesohaline reach of the Chesapeake Bay, but which experience contrasting levels of summer oxygen depletion and consequently support different degrees of bioturbation. We report on contrasting spatial and temporal distribution of these key benthic thiotrophs based on a combination of 16S rRNA gene amplicon sequencing and microscopy. Furthermore, we propose the environmental factors controlling their biomass accumulation based on biogeochemical characterization measured in this study.

## Materials

### Study sites and sediment collection

Chesapeake Bay is a large and highly productive drowned river estuary, subject to numerous past studies as a model system for studying biogeochemical consequences of eutrophication and oxygen depletion (Kemp et al. 2005). A steep-sided depression, 20–30 m in depth, cut by the relict Susquehanna River forms the main channel with an approximate north-south orientation. The main channel is strongly stratified and these mesohaline bottom waters experience recurrent, prolonged, summer oxygen depletion, and detectable bottom water sulfide (Findlay et al. 2015) and consequently support an extremely depauperate benthic fauna. The main channel is flanked by expansive shoals (Baywide mean depth: 6.5 m), which are better ventilated by surface waters, with bottom waters here experiencing only intermittent and less severe oxygen depletion. Sediments support populations of small bivalves and oligochaete worms typical of the eutrophic estuarine conditions (Sturdivant et al. 2012). We sampled stations “Central” (CB4.3C) and “West” (CB4.3W) to represent these contrasting conditions in bottom water oxygenation and bioturbation (Supporting Information Fig. S1; Table 1). Both stations are depositional environments; the sediments are fine-grained and organic carbon content is 3%–4% (Zimmerman and Canuel 2002).

Replicate sediment cores were collected using a gravity corer (Uwitec; clear PVC liners,  $\varnothing = 8.6$  cm), kept in the dark at bottom water temperature in a water bath, and transported back to the laboratory, where they were held in a climate-controlled room. From each station, one sediment core was subsampled for nucleic acids, microscopy, and chlorophyll *a* (Chl *a*) analyses, two cores were used for microsensor

**Table 1.** Site descriptions, based on data collected biweekly–monthly between 1984 and 2018, as reported by the Chesapeake Bay Program Water Quality Database (<https://www.chesapeakebay.net/what/data>). The mean ( $\pm \sigma$ ) for temperature, salinity, and dissolved oxygen are reported from bottom water measurements. Temperature is reported for the coldest (February) and warmest (August) months, and bottom water dissolved oxygen is reported for the month with the greatest oxygen depletion (July).

Parameter	Units	Central station (CB4.3C)	West station (CB4.3W)
Latitude, longitude (NAD83)	Decimal degrees	38.55505 N, 76.42794 W	38.55728 N, 76.49402 W
Depth	m	25.8 $\pm$ 0.9	8.7 $\pm$ 0.5
Secchi depth	m	0.9 $\pm$ 0.2	1.0 $\pm$ 0.5
Temperature, annual low	°C	3.3 $\pm$ 1.8	1.6 $\pm$ 1.1
Temperature, annual high	°C	25.3 $\pm$ 0.9	26.1 $\pm$ 1.0
Salinity		19.3 $\pm$ 2.2	13.9 $\pm$ 2.9
Dissolved O <sub>2</sub> , annual low	$\mu\text{mol L}^{-1}$	8.9 $\pm$ 6.8	75.3 $\pm$ 50.1

profiling, and one core was sectioned under nitrogen atmosphere for geochemical analyses. Here we focus on results of analysis of solid-phase sulfides, microsensor profiling, microscopy, and DNA amplicon sequencing data with respect to known thiotrophs. Full community analysis of DNA amplicon sequencing data is presented elsewhere (Malkin et al. submitted).

#### Cable bacteria and Beggiatoaceae filament density

Sediment cores were sectioned at 0.5 cm increments down to 5 cm for microscopy. Samples for Beggiatoaceae enumeration were transferred to plastic petri plates and kept refrigerated (4°C) for up to 3 d prior to analysis. Sediment for cable bacteria enumeration was transferred to microfuge tubes and well mixed with 95% ethanol at 1 : 1 (v/v) using a sterilized toothpick and stored at  $-20^{\circ}\text{C}$  until analysis.

The procedure for Beggiatoaceae enumeration was adapted from Jørgensen et al. (2010). A weighed subsample (0.5 g) was suspended in 5 mL artificial seawater (Red Sea Salts,  $S = 20$ ). From this suspension, a well-mixed subsample, equivalent to an initial weight of 26.8 mg, was transferred to an Utermöhl well slide and filled completely with artificial seawater. The entire slide was systematically examined by inverted light microscopy (Zeiss AxioVert A1, equipped with an AxioCam ERc5s camera connected to a PC with Zen Pro Software). All living Beggiatoaceae encountered were enumerated and imaged at 20X for length and at 63X for diameter measurements. Filaments were identified as living Beggiatoaceae if they were motile, unpigmented, and contained refractive sulfur granules, following Jørgensen et al. (2010). Beggiatoaceae biovolume was calculated assuming a cylindrical shape for each filament. Beggiatoaceae density was expressed per volume of dry sediment using measured sediment porosity values estimated from the water content of the sediment.

To enumerate cable bacteria, cells were first detached from sediment particles using methods adapted from Lunau et al. (2005). To accomplish this, an aliquot of sediment was soaked in acetate buffer solution for 60 min to dissolve

carbonates, repeatedly washed in an NaCl solution at a concentration approximately matched to bottom water salinity (average 2%), collecting the washing supernatant each time, and then resuspended in a detergent solution (Tween 80) with 10% methanol and vortexed for 60 min to detach cells. Microbial cells were then separated from sediment particles in a density centrifugation using Nycodenz (50% wt/vol), according to Kallmeyer et al. (2008). Cells detached during the washing steps and cells associating with the aqueous layer from centrifugation were captured on a cellulose acetate filter (0.2  $\mu\text{m}$ ). Filters were kept frozen ( $-20^{\circ}\text{C}$ ) until further analysis. For microscopy, filters were thawed and sectioned by razor blade, and sections were subjected to staining. Cable bacteria were identified with fluorescence in situ hybridization (FISH) using the rRNA-targeted oligonucleotide probe DSB706 (Manz et al. 1992), which effectively targets cable bacteria *Electrothrix* and *Electronema* (Pfeffer et al. 2012; Schauer et al. 2014). Staining procedures for FISH followed standard protocols (Pernthaler et al. 2001) using 45% formamide concentration for DSB706. Hybridized filters were counterstained with 1  $\mu\text{g mL}^{-1}$  SYBR Green I. As positive and negative controls, EUB338 I-III and non-EUB (non338) probes were used, respectively, as previously described (Schauer et al. 2014). After the identity of cable bacteria was confirmed using FISH on a subset of samples, enumeration proceeded following staining by Sybr Green I. Cells were counted by epifluorescence microscopy, using a Zeiss Axio Imager 2, equipped with a Photometrics CoolSnap HQ2 camera. A minimum of 200 randomly selected fields were viewed at 630X magnification and the length of each filament encountered was measured within the field. Based on 20 randomly selected filaments, cell diameter was estimated as  $1.15 \pm 0.45 \mu\text{m}$  (mean  $\pm \sigma$ ). Some of this error captures true variability in the population, but an unknown fraction may be attributable to limitations of the epifluorescence microscopy approach for measurements at this scale. Due to this measurement uncertainty, we used a rounded estimate of 1  $\mu\text{m}$  filament diameter to estimate cable bacteria biovolume.

### Sediment Chl *a*

Sediments from the surface 0.5 cm were stored frozen ( $-20^{\circ}\text{C}$ ) in glass scintillation vials prior to Chl *a* analysis. To begin analysis, sediments were thawed, mixed well, and aliquoted into stoppered glass centrifuge tubes (Kimax). Sediments were centrifuged to remove excess water. Pigment extraction was performed on the sediment pellet, using 90% acetone solution, which was well mixed into the sediment, and then agitated by gentle sonication (28 kHz, water bath sonication at  $4^{\circ}\text{C}$ ). Extraction solvent was separated from sediment by centrifugation (2500 rpm at  $4^{\circ}\text{C}$  for 5 min) and transferred to sealed glass vials. Multiple extractions were performed and pooled until successive extractions were no longer visibly green (either two or three extractions). Remaining sediment was dried at  $60^{\circ}\text{C}$  to constant weight and weighed. During all handling, care was taken to keep samples or extraction solvent cold and to minimize exposure to light. Pigment concentration in the acetone extracts was determined colorimetrically (ThermoScientific Evolution 60S UV-Vis spectrophotometer). Chl *a* concentrations were calculated according to the empirical formula of Jeffrey and Humphrey (1975):  $\text{Chl } a = 11.85 (A_{664} - A_{750}) - 1.54 (A_{647} - A_{750}) - 0.08 (A_{630} - A_{750}) \cdot v/(V \cdot l)$ , where *A* values are the absorbance at given wavelengths, corrected for background absorbance at 750 nm; *v* is the cumulative volume of extractant (L); *V* is the sediment dry weight (g); and *l* is the cuvette pathlength (1 cm). Measured porosity was used to normalize dry weight-specific values to bulk sediment volume.

### Microsensor profiling

High-resolution microsensor profiling of  $\text{O}_2$ , pH, and free sulfide ( $\Sigma\text{H}_2\text{S}$ ) was performed on two sediment cores retrieved from each site (two sets of profiles per sediment core), using commercial microsensors operated with a motorized micromanipulator (Unisense A.S., Denmark), as previously described (Malkin et al. 2015). Microsensor profiling began upon return to the laboratory, within 6 h of core retrieval. Immediately prior to microsensor profiling, water overlying the sediments was gently bubbled with air for 1–3 h. This procedure can drive an oxidation of accumulated reductants occurring near the sediment surface, particularly during summer and fall when the deviation from bottom water conditions is greatest. For this reason, the diffusive oxygen uptake (DOU) rates should be considered as potential rates.

The dissolved oxygen sensor (50- $\mu\text{m}$  tip diameter; Unisense) was calibrated with a two-point calibration using air-saturated bottom water and an anoxic depth in sediment. The pH electrode was calibrated using three NBS buffers (pH 4, 7, and 10), and corrected for the difference between NBS and total pH scale. The  $\text{H}_2\text{S}$  sensor was calibrated with a five-point standard curve obtained using  $\text{Na}_2\text{S}$  standards.  $\Sigma\text{H}_2\text{S}$  was calculated from  $\text{H}_2\text{S}$  data, corrected for pH measured at the same depth. Porosity (*v/v*) was determined from water content and density measurements upon drying to constant weight at

$60^{\circ}\text{C}$ . We calculated porosity according to  $\beta/([1 - \beta/\rho] + \beta)$ , where  $\beta$  is the water content (as a proportion) and  $\rho$  is the estimated density of the solid-phase sediment contents. Reactive transport analysis was used to extract reaction rates from the microsensor data obtained in field sampling (Table 1) and laboratory incubations. The potential DOU ( $J_i$ ) was calculated from the oxygen depth profile near the sediment water interface using Fick's first law, according to:

$$J_i = \phi/(1 - 2\ln\phi)D_i(S, T)\partial C_i/\partial x,$$

where *i* represents the pore water constituent dissolved oxygen;  $\phi$  is the measured porosity;  $D_i$  is the diffusion coefficient specific for oxygen, calculated from salinity *S* and temperature *T* using the R package *marelac* (v2.1.10; Soetaert et al. 2020), and corrected for tortuosity following Malkin et al. (2017); and  $\partial C_i/\partial x$  is the change in concentration (*C<sub>i</sub>*) with depth (*x*), estimated just below the sediment water interface. The sulfide emergence depth was calculated as the depth at which the sulfide was first detected, using a detection limit of  $2\mu\text{M}$ , and a maximum sulfide gradient was approximated as the linear slope immediately below the sulfide emergence depth.

### Extracted pore water and solid-phase analyses

Sediment cores were sectioned under  $\text{N}_2$  atmosphere at 0.5 cm increments to 5 cm within 24 h of collection. Sediment sections were transferred to 50-mL plastic centrifugation tubes (Falcon), and pore water was extracted by centrifugation (3500 rpm for 10 min) and sampled under  $\text{N}_2$  atmosphere. The remaining solid-phase material was kept frozen ( $-20^{\circ}\text{C}$ ), sealed with  $\text{N}_2$  gas in high-barrier mylar foil bags until analysis.

Sulfide from acid-volatile sulfide (predominantly  $\text{H}_2\text{S}$  and FeS) and chromium reducible sulfur (primarily comprising elemental sulfur and pyrite) were sequentially extracted in boiling 6 N HCl (Chanton and Martens 1985) and boiling 1 M chromous chloride with 6 N hydrochloric acid solution (Canfield et al. 1986), respectively, as previously described (Gomes and Johnston 2017). Extracted sulfide was driven with an  $\text{N}_2$  carrier gas to trap vessel where it was precipitated as zinc sulfide, subsequently transformed to silver sulfide, and purified by rinsing with ammonium hydroxide (Firsching 1961). Concentrations of acid-volatile sulfide and chromium reducible sulfur were determined gravimetrically.

### 16S rRNA gene amplicon sequencing

Surface sediments (0–0.5 cm) were transferred to 5-mL cryovials, rapidly frozen in a liquid nitrogen-charged dry shipper, and stored at  $-80^{\circ}\text{C}$ . Using modular procedures adapted from Lever et al. (2015), DNA was extracted from a thawed sediment aliquot. Prior to cell lysis, carbonates were dissolved in an acetate buffer–PBS solution with gentle mixing, and soluble (extracellular) DNA was removed by washing in Tris-EDTA buffer with gentle mixing. Cell lysis was achieved by

10s vortex with sterile beads followed by heating (50°C), then a freeze-thawing cycle (−80°C, 4°C), in combination with a chemical lysis solution containing 0.5% Triton X-100 and guanidium hydrochloride adjusted to pH 10. This full lysis procedure was repeated three times. Extracted DNA was purified by two washes with a chloroform-isoamyl alcohol solution and then precipitated with a PEG 8000-NaCl solution in the presence of linear polyacrylamide at room temperature. A final wash was made in 70% ethanol, and the resultant DNA pellet was allowed to air dry and then dissolved in water. Extracted DNA quality was checked by agarose gel electrophoresis, and its concentration was measured by fluorometry (Qubit 2.0 fluorometer; Invitrogen) using Qubit dsDNA assay kits. Further purification was found to be unnecessary.

The hypervariable region V4-V5 of the 16S rRNA gene was targeted for amplification, using the modified primer pair 515F-Y/926R (GTG YCA GCM GCC GCG GTA A)/(CCG YCA ATT YMT TTR AGT TT) (Parada et al. 2015). Amplification, barcoding, and sequencing were performed at the Bioanalytical Services Laboratory (BASLAB, IMET). Amplification proceeded via two steps, first for gene amplification and the second for adding indexes, and clean-up was accomplished using AMPure XP beads (Beckman Coulter). Amplicons were sequenced using an Illumina MiSeq platform (2 × 300 nt paired-end reads).

Bioinformatic analysis was performed in *R* (v 3.6) using the *dada2* pipeline (Callahan et al. 2016), and the resultant amplicon sequence variants (ASVs) were taxonomically assigned using the “IdTaxa” function from the package *Decipher* (Murali et al. 2018), using the SILVA ribosomal small subunit database (v138; Pruesse et al. 2007). This taxonomic assignment algorithm was chosen to minimize overclassification errors. Sequences affiliated to mitochondria and chloroplasts were removed. Sequences affiliated to Eukarya or which could not be assigned to a Kingdom, and sequences which could not be assigned to a Phylum within Bacteria were assumed to be artefacts and were removed. Following this pruning, a total of ~ 1.04 million reads remained (23,500–132,000 reads per sample), representing 4270 ASVs. Statistically significant differences between categories of samples (e.g., seasons: winter + spring vs. summer + fall; stations: West vs. Central) were tested using permutational ANOVA (PERMANOVA), implemented with the *vegan* package (v 2.5.2, CRAN) (Oksanen 2019). To assess if ASVs affiliated with cable bacteria were differentially represented between sites and seasons, we used the differential expression analysis software tool *DeSeq2* (Love et al. 2014). A phylogenetic tree was constructed using full length 16S rRNA gene sequences obtained from NCBI nucleotide database affiliated to *Candidatus Electrothrix* and *Candidatus Electronema* together with representatives from the closely related genera *Desulfobulbus* and *Desulfovibrio*, and *Desulfobacter postgatei* as an outgroup. Sequences were aligned using DECIPHER (Wright 2015), and then trees were constructed using a maximum-likelihood procedure implemented

by the program Randomized Accelerated Maximum Likelihood (RAXML v. 8.2.10; Kozlov et al. 2019). Maximum likelihood tree topology was optimized using the generalized time-reversible model of nucleotide substitution with the CAT rate variation approximation and a random seed as a starting point using the autoMRE algorithm to optimize bootstrapping recurrence. ASVs assigned to *Candidatus Electrothrix* and *Candidatus Electronema* were selected from our dataset and aligned to the tree using *PaPaRa* (Berger and Stamatakis 2011) and placed on the tree using the package *EPA-ng* (Barbera et al. 2019). Data visualization and statistic calculations were accomplished using the package *phyloseq* (v. 1.24.2; McMurdie and Holmes 2013) and *ggtree* (Yu et al. 2017).

## Results

### Seasonal bottom water conditions

At the Central Station, bottom waters were hypoxic (< 2 mg L<sup>-1</sup>; 62.5 μmol L<sup>-1</sup>) from June through September in 2017 (Fig. 1A) or October in 2018 (Fig. 1B). Minimum dissolved oxygen concentrations were 13 and 9 μM in 2017 and 2018, respectively, based on the biweekly sampling (Chesapeake Bay Program Water Quality Database; Supporting Information Fig. S2). At the West Station, hypoxic bottom waters were reported during May, June, and/or July, but not in consecutive months, consistent with frequent ventilation of bottom waters. Minimum dissolved oxygen concentrations were 25 and 19 μmol L<sup>-1</sup> in 2017 and 2018, respectively (Chesapeake Bay Program Water Quality Database; Supporting Information Fig. S3). The bottom water dissolved oxygen and temperature values from these years were typical of those reported since 1984 (Supporting Information Figs. S2, S3). Additional bottom water quality parameters (temperature, salinity) measured at the time of sampling are reported in Supporting Information Table S1.

### Sediment chlorophyll

Chl *a* concentrations at the sediment surface on most occasions were relatively low and varied little with season (Fig. 1C, D), except for one value from the Central Station in May 2018, where sediment Chl *a* was 0.81 nmol Chl *a* cm<sup>-3</sup>. Excluding this elevated value, the surface sediment Chl *a* values were 0.21 ± 0.03 nmol Chl *a* cm<sup>-3</sup> (mean ± sd; *n* = 8) at West Station and 0.11 ± 0.03 nmol Chl *a* cm<sup>-3</sup> (*n* = 7) at Central Station.

### Acid volatile sulfide and chromium reducible sulfur inventories

Strong seasonality in surface sediment acid-volatile sulfide inventories were observed at both sites, and no significant differences were detected between sites (Fig. 1E,F). Sulfide from acid-volatile sulfide was not detected at the sediment surface during winter and spring and was up to 227 μmol S cm<sup>-3</sup> during summer. Sediment chromium reducible sulfur concentrations were higher on average at West Station (mean ± σ:

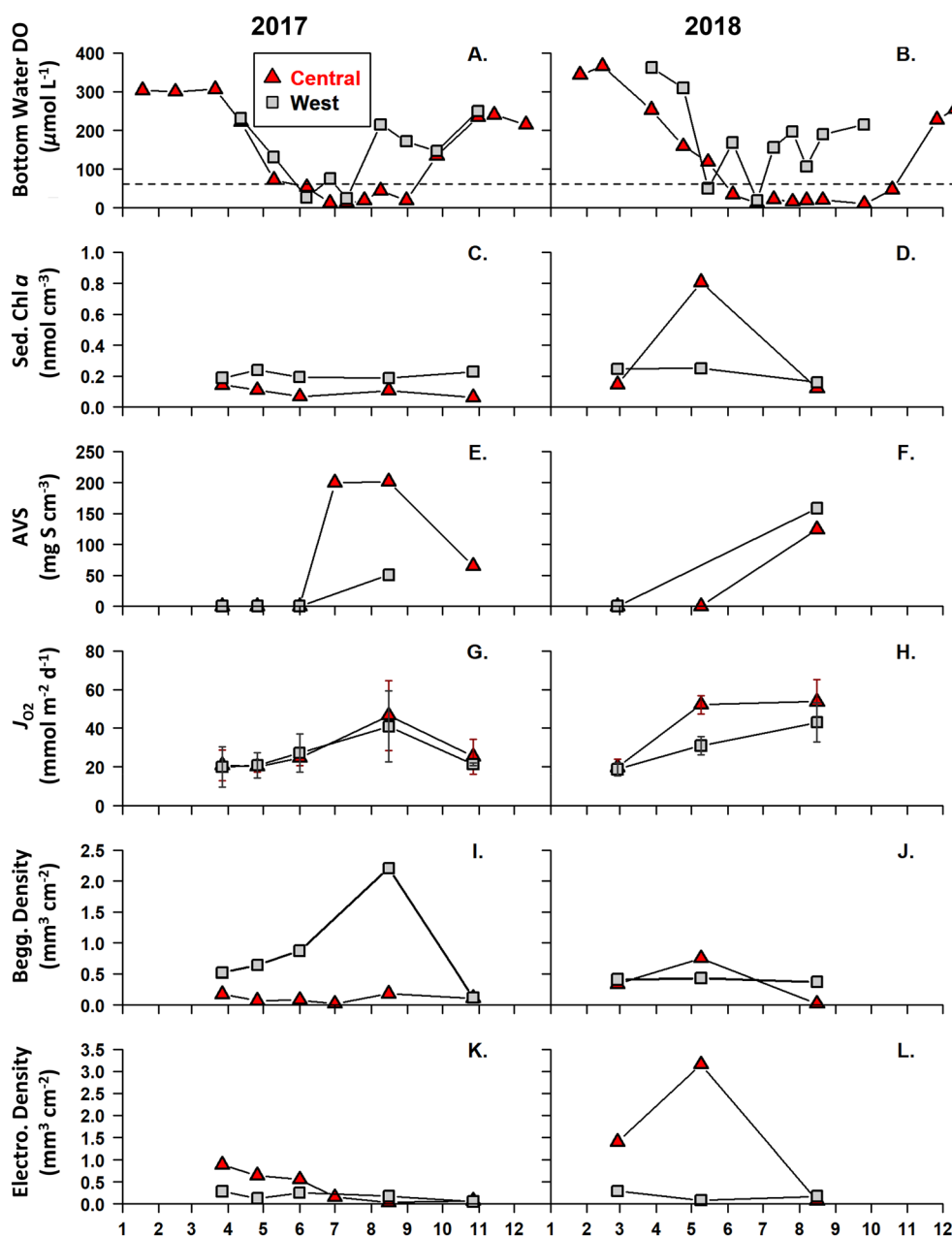


**Fig. 1.** Seasonal sediment conditions and densities of filamentous sulfur-oxidizing bacteria, measured at a site in the seasonally anoxic main channel (“Central”) and the western shoal (“West”). Bottom water dissolved oxygen concentrations (“Bottom Water DO”;  $\mu\text{mol L}^{-1}$ ), reported by the Chesapeake Bay Water Quality Program for (A) 2017 and (B) 2018. Dashed line indicates hypoxia ( $2 \text{ mg L}^{-1} = 62 \mu\text{mol L}^{-1}$ ). Surface sediment chlorophyll *a* concentrations (“Sed. Chl *a*”; 0–1 cm;  $\text{nmol cm}^{-3}$ ) in (C) 2017 and (D) 2018. Concentrations of acid-volatile sulfide (“AVS”) in surface sediment (0–1 cm;  $\mu\text{mol S cm}^{-3}$ ) in (E) 2017 and (F) 2018. Potential flux of dissolved oxygen into sediments (“ $J_{\text{O}_2}$ ”;  $\text{mmol m}^{-2} \text{d}^{-1}$ ) as determined from microsensors profiles, with standard deviation reported from four profiles in (G) 2017 and (H) 2018. Areal densities of Beggiatoaceae; “Begg. Dens.”;  $\text{mm}^3 \text{cm}^{-2}$ ) in (I) 2017 and (J) 2018. Areal densities of cable bacteria (“Electro. Dens.”;  $\text{mm}^3 \text{cm}^{-2}$ ) in (K) 2017 and (L) 2018.

$538 \pm 250 \mu\text{mol S cm}^{-3}$ ) than at Central Station ( $450 \pm 64 \mu\text{mol S cm}^{-3}$ ). The chromium reducible sulfur inventories integrated to 2 cm were significantly higher at West Station compared with Central Station ( $t = 9.483$ ,  $df = 6$ ,  $p < 0.01$ ; Supporting Information Fig. S4).

#### Microsensor profile distributions

Potential DOU varied seasonally, ranging at the Central Station between  $19.8 \pm 4.3 \text{ mmol m}^{-2} \text{d}^{-1}$  (March) and  $53.8 \pm 11.4 \text{ mmol m}^{-2} \text{d}^{-1}$  (August), and at the West Station between  $18.7 \pm 3.4 \text{ mmol m}^{-2} \text{d}^{-1}$  (March) and  $43.0 \pm$

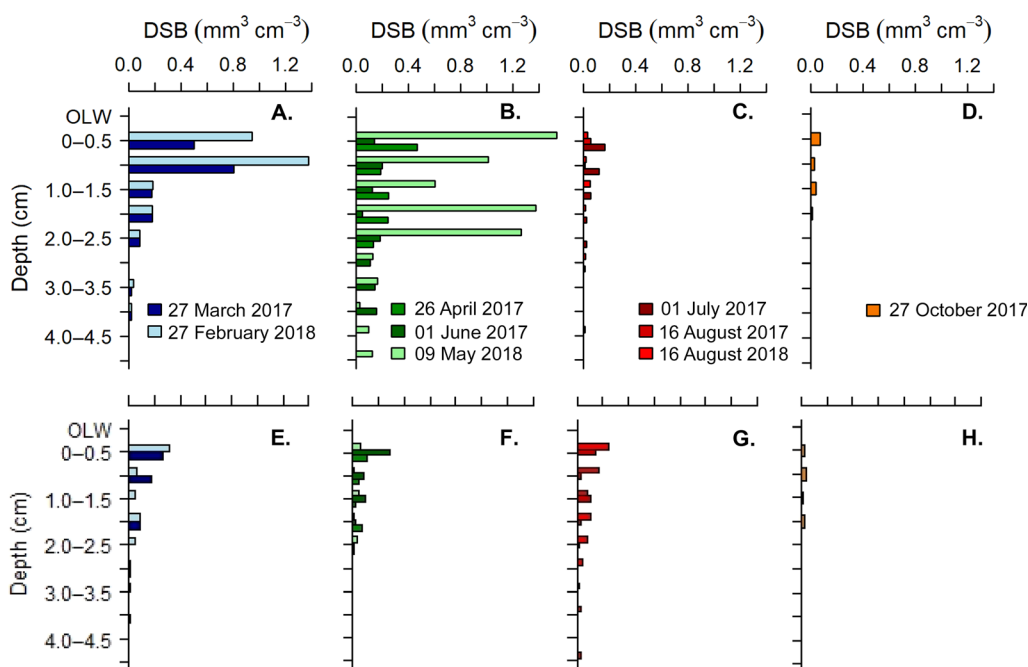


**Fig. 2.** Depth distribution of cable bacteria biovolume in (A,E) winter; (B,F) spring; (C,G) summer; and (D,H) fall. Top panels from Central Station and bottom panels from West Station. DSB indicates cable bacteria, counted with the DSB706 oligoprobe; OLW here refers to overlying water immediately above sediment surface.

10.1 mmol m<sup>-2</sup> d<sup>-1</sup> (August) (Fig. 1G,H). Detectable differences were not observed between sites on most dates, except in May 2018, when potential diffusive oxygen flux was elevated at Central Station to  $52.2 \pm 4.8$  vs.  $31.0 \pm 4.7$  mmol m<sup>-2</sup> d<sup>-1</sup> at West Station ( $t = 21.786$ ,  $df = 6$ ,  $p < 0.001$ ).

At the Central Station, microsensor profiles revealed seasonal patterns indicative of cable bacteria activity (i.e., an anodic pH minimum near the horizon of sulfide accumulation and occasionally a cathodic pH maximum in the oxic zone) during winter and spring (February, April, May, June), coinciding with the months when cable bacteria density was greater than 0.5 mm<sup>3</sup> cm<sup>-2</sup> (Supporting Information Fig. S5). The most extreme pH minimum was observed in May 2018 (pH 6.26), coinciding with the highest cable bacteria density (see Fig. 1K,L). Samples from June 2017 and February 2018 most clearly exhibited a pH minimum coinciding with the sulfide emergence horizon (Supporting Information Fig. S5). In most months when cable bacteria density was near detection limits, pH profiles did not exhibit a local minimum. In March and October 2017, there were small local pH minima, similar to profiles indicative of ferrous iron oxidation (Seitaj et al. 2015). The typology of sulfide oxidation by nitrate-accumulating Beggiatoaceae was not observed among the profiles from either station (*sensu* Sayama et al. 2005; Seitaj et al. 2015). At the West Station, a pH minimum was always evident just below the oxic zone. This horizon shifted with season, shoaling in the warmer months in concert with the oxygen penetration depth

(Supporting Information Fig. S6), and matching the typology for the cycling of iron between reduced and oxidized mineral forms associated with solid-phase mixing (Seitaj et al. 2015).

At the Central Station, sediment pore water sulfide exhibited strong seasonal oscillations. In winter, values were below detection limits (in upper 4 cm), while in spring (e.g., April) a sulfide emergence depth was observed at 3.3 cm with a maximum sulfide gradient of 1.3  $\mu\text{mol L}^{-1} \text{mm}^{-1}$  (Supporting Information Fig. S5). In summer, a suboxic zone was lost entirely, and a maximum sulfide gradient of 150  $\mu\text{mol L}^{-1} \text{mm}^{-1}$  was observed, with concentrations in excess of 2 mmol L<sup>-1</sup> by 4 cm. At the West Station, sulfide was not detected in the upper 4 cm in winter-spring, becoming detectable in the summer, though at lower concentrations than Central Station. The sulfide profiles were exceptionally high in August 2018 at West Station, with free sulfide becoming detectable by 0.5 cm, and reaching 100  $\mu\text{mol L}^{-1}$  by 3 cm depth (Supporting Information Fig. S6).

#### Cable bacteria densities (microscopy results)

At the Central Station, depth-integrated cable bacteria density declined from winter (e.g., 1.4 mm<sup>3</sup> cm<sup>-2</sup> in February 2018) to summer (e.g., 0.03 mm<sup>3</sup> cm<sup>-2</sup> in August 2017; Fig. 1K,L). The highest densities of cable bacteria were usually observed in the top 1 cm of sediment (Fig. 2). In addition to this seasonality, there was a remarkable elevation of cable

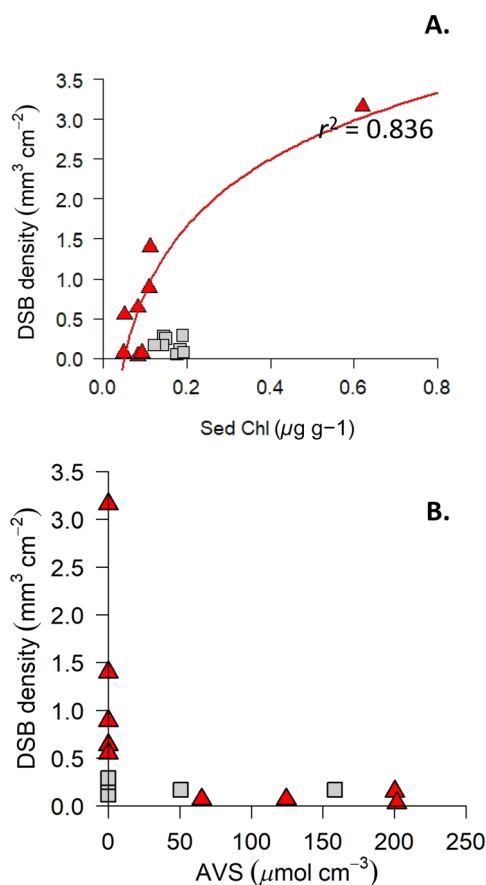


**Fig. 3.** Relationships between (A) sediment chlorophyll (“Sed Chl  $a$ ”) and cable bacteria density (DSB, counted with the DSB706 oligoprobe) and (B) sediment acid-volatile sulfide (AVS) and cable bacteria density. The relationship between sediment chlorophyll and cable bacteria density at Central Station is fit with a natural log-linear curve (DSB density =  $1.2069 \cdot \ln(\text{Chl } a) + 3.28$ ).

bacteria density observed in May 2018 at the Central Station ( $3.2 \text{ mm}^3 \text{ cm}^{-2}$ ; Fig. 11). At this time, elevated cable bacteria densities were observed from the sediment surface down to 2.5 cm (cumulative length per volume:  $368 \pm 116 \text{ m cm}^{-3}$ ), with lower densities observed below this depth ( $33 \pm 15 \text{ m cm}^{-3}$ ; Fig. 2). Depth-integrated cumulative length was  $1005 \text{ m cm}^{-2}$ . Cable bacteria were also observed at the West Station, though at lower density (maximum:  $0.4 \text{ mm}^3 \text{ cm}^{-2}$  or  $124 \text{ m cm}^{-2}$  in August 2018).

Cable bacteria density was positively correlated with sediment Chl  $a$ , described by a log-linear curve (Fig. 3A). Acid-volatile sulfide was nondetectable in surface sediments when cable bacteria were abundant (Fig. 3B).

### Beggiatoaceae biovolume and distribution

The depth-integrated biovolume of Beggiatoaceae was typically lower at the Central Station ( $0.02\text{--}0.34 \text{ mm}^3 \text{ cm}^{-2}$ ) than at the West Station ( $0.12\text{--}2.21 \text{ mm}^3 \text{ cm}^{-2}$ ; Fig. 11J), except

during May 2018 when unusually high values were observed at the Central Station ( $0.75 \text{ mm}^3 \text{ m}^{-2}$ ). Beggiatoaceae depth distribution varied seasonally. Beggiatoaceae filaments were generally confined to shallower maximum depths at the Central Station than the West Station, and filaments generally occupied deeper depths in winter and spring than during summer and fall (Fig. 4). In the summer months only, Beggiatoaceae was visible at the sediment surface at both sites, appearing as a thin white film. Distribution of Beggiatoaceae diameters at both sites was multimodal, with modes (mean  $\pm$  SD) at  $5.3 \pm 0.6$ ,  $12.6 \pm 1.3$ , and  $18.9 \pm 4.0 \mu\text{m}$ . A relationship was observed between the potential DOU and Beggiatoaceae density among samples in which the sulfide emergence depth was greater than 1.0 cm ( $n = 11$ , Pearson correlation  $r = 0.5918$ ,  $p < 0.05$ ), but not among samples in which the sulfide emergence depth was shallower than 1.0 cm (Fig. 5).

### Identification of sulfur-oxidizing bacteria based on 16S rRNA gene sequences

ASVs affiliated with marine cable bacteria (*Candidatus Electrothrix*) were detected in all winter and spring samples (both stations) and in none of the samples from summer and fall. Cable bacteria ASVs were observed at a higher relative abundance at the Central Station (typically 0.7–1.2%, and exceptionally to 3.6% during May 2018) than at the West Station (0.04–0.12%; Fig. 4). PERMANOVA analysis confirmed differences in community composition between the stations were significant ( $p < 0.001$ ), and *DeSeq2* analysis confirmed that *Candidatus Electrothrix* was found at significantly higher proportion at the Central Station than the West Station ( $\alpha = 0.01$ ).

One *Candidatus Electrothrix* ASV (ASV\_0123), which was most closely affiliated to *Candidatus Electrothrix communis* (Supporting Information Fig. S7), was dominant in terms of both relative abundance and prevalence across samples at both sites (Fig. 6). The sediment sample collected in May 2018 from Central Station stands out for having the highest proportion of cable bacteria ASVs (3.6% of all reads), and for exhibiting the greatest phylotype diversity among cable bacteria (5 ASVs each constituting more than 0.1% of all sequence reads; Fig. 6). Two of the other ASVs assigned to *Candidatus Electrothrix* were affiliated most closely to *Candidatus Electrothrix marina* (Supporting Information Fig. S7). Other ASVs that were assigned to *Candidatus Electrothrix* could not be resolved to species level. One ASV appeared to be misassigned, with ASV\_2881 exhibiting greater affiliation to *Desulfobulbus*, and was not considered in the sum of cable bacteria relative abundance.

Direct counts of cable bacteria were significantly correlated with percentage *Candidatus Electrothrix* reads at the Central Station ( $r = 0.962$ ,  $df = 8$ ,  $p < 0.001$ ; Supporting Information Fig. S8). As anticipated, based on the presence of introns in their 16S rRNA genes (Salman et al. 2012), no correlations

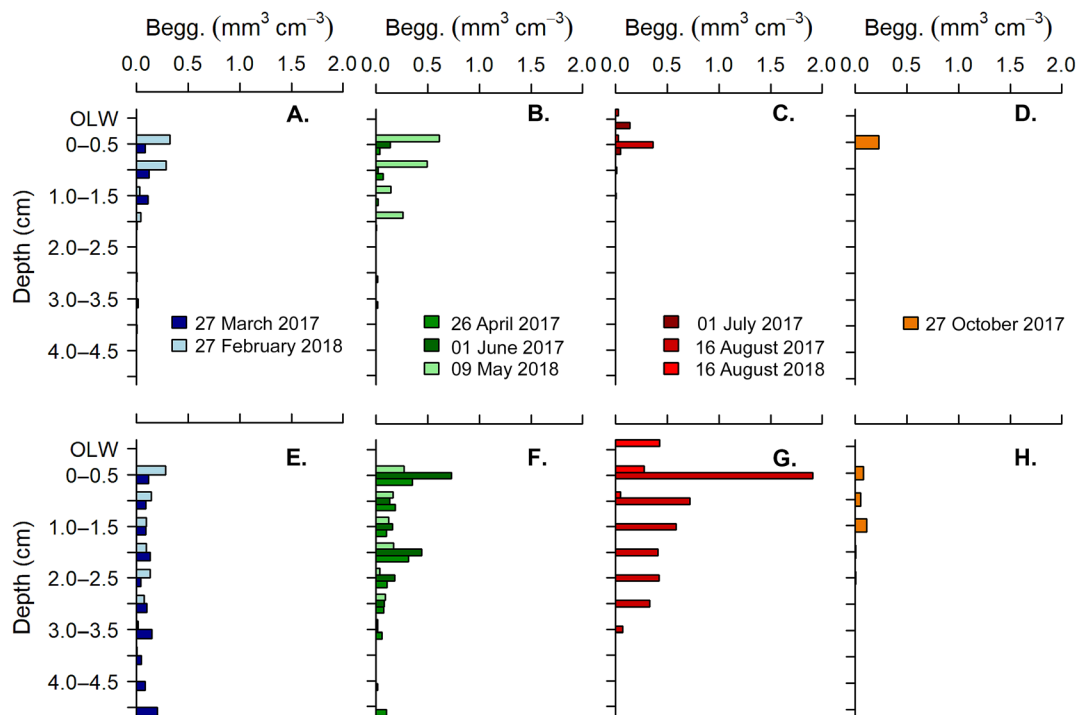


**Fig. 4.** Depth distribution of Beggiatoaceae biovolume in (A,E) winter; (B,F) spring; (C,G) summer; and (D,H) fall. Top panels (A–D) from Central Station and bottom panels (E–H) from West Station.

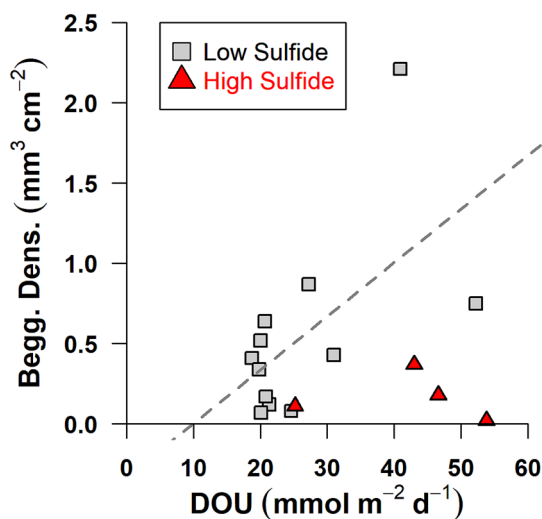


**Fig. 5.** Relationships between potential diffusive oxygen uptake (“DOU”) and density of Beggiatoaceae (Begg.) filaments, fit with a linear regression ( $\text{Begg. Density} = 0.033 * (\text{DOU}) - 0.333$ ). The relationship between potential DOU and Beggiatoaceae density is significant among samples where sulfide was below detection in the upper cm of sediment (“Low Sulfide”; Pearson correlation = 0.5918;  $p = 0.043$ ,  $n = 11$ ). Beggiatoaceae density among samples with sulfide detected in the top 1 cm of sediment (“High Sulfide”) exhibit no relationship with DOU.

were found between direct counts of Beggiatoaceae filaments and any individual ASV or agglomerations of related ASVs affiliated with Beggiatoales.

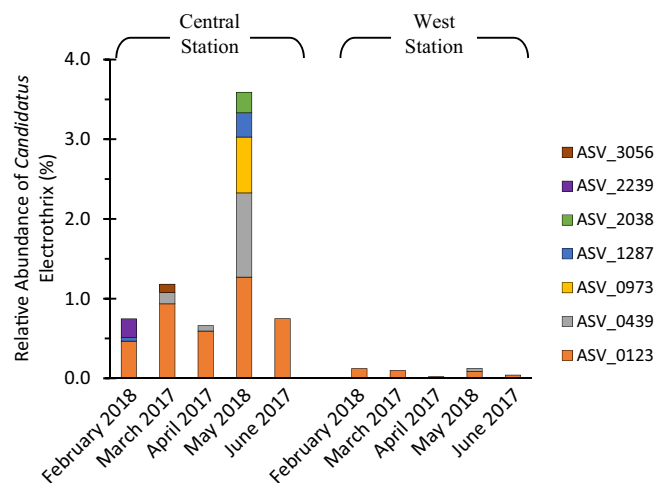


**Fig. 6.** Relative abundance of *Candidatus Electrothrix* in Chesapeake Bay sediment, during months when it was detected (February–June). Bars are organized by month, without regard to year. Each series represents a unique ASV affiliated to *Candidatus Electrothrix*.

## Discussion

### Distribution of cable bacteria

The densities of cable bacteria observed in this study were in the range previously reported from *ex situ* cores of sulfide-generating sediments. At the seasonally anoxic Central Station, densities were 174–447  $\text{m cm}^{-2}$  during most dates between winter and spring, with an exceptional peak of

1005 m cm<sup>-2</sup> co-occurring with elevated sediment Chl *a* in May 2018. Densities in these high ranges have been previously reported from other productive coastal marine sites that lack high densities of large bioturbating infauna due to seasonal hypoxia or sulfide accumulation, including Grevelingen, a restricted coastal basin of the North Sea (402–480 m cm<sup>-2</sup>) (Seitaj et al. 2015); intertidal bivalve reefs (58–1038 m cm<sup>-2</sup>) (Malkin et al. 2017); and a depositional zone of the North Sea (168–352 m cm<sup>-2</sup>) (van de Velde et al. 2016). Lower densities have been reported from systems with lower oxygen availability, including the Baltic Sea ( $\leq 33$  m cm<sup>-2</sup>) (Marzocchi et al. 2018), potentially reflecting a constraint imposed by low oxygen availability (Burdorf et al. 2018).

At the bioturbated West shoal station, cable bacteria were observed, but always at lower density than at the Central Station (16–124 m cm<sup>-2</sup>). These densities are similar to those reported from sulfide-generating heavily bioturbated intertidal sands ( $\leq 56$  m cm<sup>-2</sup>) (Malkin et al. 2017), from a sulfide-generating bioturbated sediment of a mangrove swamp (77 m cm<sup>-2</sup>) (Burdorf et al. 2016), and from seasonally hypoxic stations of the Baltic that support modest bioturbation by macrofauna ( $\sim 70$ –150 m cm<sup>-2</sup>) (Hermans et al. 2019).

#### Constraints on cable bacteria: Electron donor supply

The seasonality of cable bacteria reported at Central Station is in close agreement with that previously observed in Grevelingen (Seitaj et al. 2015), providing evidence that winter–spring dominance is likely a general feature of their ecology among seasonally hypoxic systems. Previous work has identified three sources of sulfide to cable bacteria: the upward diffusive flux of sulfide originating from sulfate reduction occurring below the suboxic zone; sulfide produced cryptically by sulfate reduction occurring within the suboxic zone; and acidic dissolution of iron monosulfides (FeS) also occurring within the suboxic zone (Risgaard-Petersen et al. 2012). The relative importance of these sources appears to depend on the availability of FeS (Larsen et al. 2014), and the exhaustion of the FeS pool may underlie the frequent observation that cable bacteria populations reach an unsustainable maximum during time course incubation studies (Schauer et al. 2014; Rao et al. 2016), although alternative physiology-based hypotheses have also been proposed (Kjeldsen et al. 2019), and predation control has not been extensively explored. Our dataset is consistent with a conceptual model that a baseline seasonality of cable bacteria in Chesapeake Bay is supported by a seasonally replenished FeS stock in near-surface sediments.

The density of cable bacteria reported here also reinforces the role of cable bacteria as quick responders and efficient scavengers of free sulfide (Malkin et al. 2017). In May 2018 at Central Station, a spike was observed in sediment Chl *a*, which was accompanied by an large increase in both cable bacteria density and diversity, and an increase in Beggiatoaceae. Diatom blooms occur frequently in Chesapeake Bay during spring (Harding et al. 2015), and this was the most likely source of the

particular hotspot encountered in this study. Previous estimates of sulfate reduction in the central channel found that spring phytodetritus stimulated sulfate reduction in the upper 2 cm of the sediment (Marvin-DiPasquale et al. 2003). The spike in sediment Chl *a* and thiotroph biomass observed in this study was notably accompanied by an increase in microbial activity, but not in sulfide accumulation.

This hypothesized cryptic sulfur cycling associated with a spring phytoplankton bloom may be widespread across other restricted coastal basins as well. Phytodetritus influx to surface sediments following a phytoplankton spring bloom have been reported from Long Island Sound (e.g., Sta. P in Aller and Cochran 2019), and stimulation of sulfate reduction in the upper sediment (0.2–1.0 cm) in response to a deposited spring bloom has also been previously reported from Aarhus Bay (Moeslund et al. 1994; Thamdrup et al. 1994). Furthermore, the organic detritus to the seafloor resulting from spring blooms may be more labile than organic matter inputs at other times of the year (Rodil et al. 2020). We sampled surface sediment from the main channel of Chesapeake Bay again in May 2019, but did not observe a spike in Chl *a* at the sediment surface, nor a bloom of Beggiatoaceae and cable bacteria (based on microscopy; Malkin unpub. data). These observations suggest that the persistence of the spring bloom phytodetritus may be short-lived (Graf 1989; Lehto et al. 2014), variable between years, or heterogeneously distributed. Jiang and Xia (2017) reported that the timing and intensity of the spring bloom in Chesapeake Bay varies interannually and is a function of wind field and Susquehanna River discharge. The rapid colonization by diverse thiotrophs (including *Candidatus Electrothrix*, Beggiatoaceae) when oxygen and nitrate are available in the surface sediments appears to suppress the transport of sulfide generated by sulfate reduction near the sediment surface into the water column during spring blooms.

The diversity of cable bacteria and their biogeography is just beginning to be unravelled. *Candidatus Electrothrix* has been described as the marine genus of cable bacteria and *Candidatus Electronema* as the freshwater genus (Trojan et al. 2016), and their niche partitioning based on salinity has been recently confirmed (Dam et al. 2021). Employing catalyzed reporter deposition FISH (CARD-FISH) with species-specific oligoprobes, Marzocchi et al. (2018) reported a mix of *Candidatus Electrothrix* species, among *Ca. E. marina*, *Candidatus Electrothrix aarhusiensis*, and *Ca. E. communis*, coexisting in Baltic Sea sediments. Here, we report that winter and spring samples were dominated by a single ASV most likely affiliated to the species *Ca. E. communis*, which also vastly dominates in laboratory incubations (Liau, unpub. data). By contrast, the profusion of *Candidatus Electrothrix* in May 2018 was comprised of multiple *Candidatus Electrothrix* phylogenotypes which could not be confidently assigned to species. The elevated diversity during the spring bloom indicates not only the co-existence of multiple taxa in these sediments, but also that the rate of sulfide supply may be an important factor

in the niche partitioning between *Candidatus Electrothrix* phylotypes or species. The stable relative proportion of the ASV affiliated to *Ca. E. communis* during this period of elevated activity also suggests varying constraints on different cable bacteria populations operating concurrently. An analysis of cable bacteria species distribution by Dam et al. (2021) reveals *Ca. E. communis* to be widespread in fresh and brackish habitats, and has not been reported from high salinity environments. It seems plausible that this species may be particularly well adapted to estuarine environments, though more data would be needed to test this hypothesis.

#### **Constraints on cable bacteria: Electron acceptor availability (oxygen, nitrate)**

Cable bacteria can use oxygen and nitrate as electron acceptors for cathodic reduction (Nielsen et al. 2010; Marzocchi et al. 2014). Laboratory experiments (Burdorf et al. 2018) and field data (Marzocchi et al. 2018; Hermans et al. 2019) have demonstrated that depleted bottom water oxygen concentrations can constrain cable bacteria density, which may be particularly relevant in systems with persistent interannual oxygen depletion. Likewise, on a seasonal basis, oxygen depletion likely severely restricts cable bacteria growth in the central channel in Chesapeake Bay. On an annual basis, we must also consider how bottom water oxygen levels indirectly impact cable bacteria through their influence on the presence and absence of bioturbating macrofauna. A suppression of infauna through severe seasonal oxygen starvation appears to provide the conditions that promote the proliferation of cable bacteria at the sediment surface in this dataset. Similar to other locations (Seitaj et al. 2015), the spatial extent and severity of oxygen depletion in Chesapeake Bay therefore likely affects the system-level cable bacteria density through its influence not only on sulfide availability, but also on benthic fauna, with consequences for biogeochemical cycling.

#### **Constraints on cable bacteria: Bioturbation**

Cable bacteria were observed at the bioturbated West Station but had persistently 1–2 orders of magnitude lower cell density than at the Central Station. In previous work, we observed a negative relationship between bioturbation and cable bacteria abundance and proposed that bioturbation may negatively influence the growth of cable bacteria through sediment overturning, by directly altering the simultaneous access of the bacterial filaments to electron donors and acceptors, and/or by direct mechanical breakage (Malkin et al. 2015). Our results here broadly support the conclusion that bioturbation creates conditions that inhibit cable bacteria and enable other bacteria including Beggiatoaceae to outcompete cable bacteria, at least in proximity to the sediment surface. While the specific mechanism(s) driving the differences in cable bacteria abundance between the sites is not entirely clear, it is well established that bioturbation strongly influences the sediment inventories of oxidants and reductants (Kristensen and

Kostka 2005; Braeckman et al. 2010; Rao et al. 2014) and exerts a major influence on the microbial activity and community structure in sediments (Papasprou et al. 2006; Jochum et al. 2017; Booth et al. 2019). One plausible driver of the difference is the lower free sulfide availability at the West Station. Although sulfate reduction rates previously reported in these bioturbated sediments were similar or higher at the West Station than at the Central Station (Roden and Tuttle 1993), and winter acid-volatile sulfide inventories were not detectably different between the stations, the two stations did strongly differ in their free sulfide accumulation. This is most evident in samples from July, August, and October, when for example, sulfide concentrations at 3 cm depth reached between 700 and 1700  $\mu\text{mol L}^{-1}$  at Central Station, vs. 20–30  $\mu\text{mol L}^{-1}$  at West Station (Supporting Information Figs. S5, S6). Although sulfide may be generated at similar rates (or even higher at the West Station; Roden and Tuttle 1993), the sites differ in the composition of dominant sulfur-oxidizing bacteria, free sulfide concentrations, and chromium reducible sulfur inventories. This implies that between-site variation in water column chemistry, sediment characteristics, and the extent of bioturbation impacts rates and pathways of sulfur oxidation and chromium reducible sulfur formation, though the latter remains to be tested.

It remains a possibility that the burrows of infauna may be punctuated with ecologically important hotspots of cable bacteria that were not captured with our sampling approach. Aller et al. (2019) reported locally high densities of cable bacteria associated with parchment worm burrows, which are stable on the order of weeks. Similarly, Martin et al. (2019) observed enrichment of cable bacteria in association with the fine root hairs of growing seagrasses, and Scholz et al. (2021) reported cable bacteria associated with rhizospheres of aquatic plants occurring to deeper depths than in areas without vegetation. In each of these studies, the authors suggested that as efficient scavengers of sulfide, cable bacteria may provide a benefit to the animals and plants they live in association with by maintaining burrows or rhizospheres free of free sulfide. In support of the hypothesis that cable bacteria may grow to deeper depths in bioturbated sediments (albeit with potentially greater spatial heterogeneity), we obtained amplicon sequences from multiple depths in May 2018 at 0–1, 5–6, 10–11, 20–21, and 30–31 cm intervals. These samples revealed *Candidatus Electrothrix* were confined to near the surface at the Central Station, but were detectable to 10 cm depth at the West bioturbated station (Supporting Information Fig. S9). These data lend support to the hypothesis that cable bacteria could be important for removing sulfide at depth in sediment and play an important ecological function even where not highly abundant at the sediment surface, though we caution that the DNA signatures of cable bacteria may not necessarily reflect living cable bacteria or their activity. The activity of the cable bacteria DNA detected at 10 cm depth is unknown and could be an inactive relic mixed from shallower sediment by

bioturbation. Other markers of activity (e.g., RNA transcripts) would be useful for further addressing their realized role in bioturbated sediments.

### Beggiatoaceae: Distribution, constraints, and contribution to sulfur oxidation

Beggiatoaceae in mesohaline Chesapeake Bay were most often distributed throughout suboxic sediment layers. They were found to at least 4 cm (the maximum depth examined) at the bioturbated station. Although frequently reported as conspicuous mats forming at the surface of sediments with advective sulfide flow (Jørgensen and Boetius 2007), this more inconspicuous subsurface distribution is typical of sulfide-generating subtidal coastal systems (Mußmann et al. 2003; Jørgensen et al. 2010; Seitaj et al. 2015). Maximum depth-integrated densities encountered in this study occurred at the bioturbated station in August 2017 ( $2.2 \text{ mm}^3 \text{ cm}^{-2}$ ). Applying the same density and volume conversion factors used in the present study, our Beggiatoaceae density estimates are similar to those reported from Limfjorden ( $1.4\text{--}1.6 \text{ mm}^3 \text{ cm}^{-2}$ ) (Mußmann et al. 2003), and from a seasonally hypoxic station in Grevelingen (winter–summer  $< 0.1$ ; fall =  $2.2\text{--}7.5 \text{ mm}^3 \text{ cm}^{-2}$ ) (Seitaj et al. 2015), and about an order of magnitude higher than densities observed in Arctic marine sediments ( $0.1\text{--}0.3 \text{ mm}^3 \text{ cm}^{-2}$ ) (Jørgensen et al. 2010).

Beggiatoaceae biovolume was positively correlated with the potential DOU among samples lacking sulfide accumulation in the upper centimeter of sediment. Conversely, Beggiatoaceae biovolume was unrelated to potential DOU among samples with sulfide emergence depths shallower than 1 cm. The distribution of Beggiatoaceae is frequently heterogeneous and the drivers that underlie its distribution remain unconstrained. Based on the distribution we observed, we hypothesize that the Beggiatoaceae in Chesapeake Bay find a niche where there is sufficient sulfate reduction to provide sulfide for their growth, yet sufficient bioturbation to minimize high sulfide levels in proximity to the sediment surface. Previous studies have shown that Beggiatoaceae exhibit chemotaxis away from free sulfide accumulation (Dunker et al. 2010), despite using this reduced compound as an electron donor. These conditions are met in the fine-grained sediments on the mesohaline shoal in Chesapeake Bay. Further surveys will be needed to better constrain their distribution.

We sought to calculate whether Beggiatoaceae could account for the rates of sulfide oxidation likely occurring in the sediments at West Station, where their biovolume was greatest. To do this, we estimated the maximum potential sulfide turnover by Beggiatoaceae filaments, based on their maximum measured density (August 2017 at West Station). We assumed their sulfide oxidation is coupled to dissimilatory nitrate reduction to ammonium ( $\text{HS}^- + \text{NO}_3^- + \text{H}^+ + \text{H}_2\text{O} \rightarrow \text{SO}_4^{2-} + \text{NH}_4^+$ ). Preisler et al. (2007) measured a biomass-specific nitrate turnover by Beggiatoaceae of  $\sim 13 \text{ mmol L}^{-1} \text{ d}^{-1}$  at  $15^\circ\text{C}$ . At the time of peak biomass bottom water temperature was  $\sim 25^\circ\text{C}$ .

Applying a Q10 value of 2 and 1 : 1 stoichiometry, this would yield a biomass-specific rate of sulfide oxidation of  $26 \text{ mmol L}^{-1} \text{ d}^{-1}$ . At the maximum biomass density of  $1.9 \text{ mm}^3 \text{ cm}^{-3}$  observed, this would be equivalent to a maximum sulfide oxidation rate of  $49.4 \text{ nmol cm}^{-3} \text{ d}^{-1}$ . Roden and Tuttle (1993) measured sulfate reduction rates using the  $^{35}\text{S}$  method in surface sediments near the West Station in August at  $600\text{--}900 \text{ nmol cm}^{-3} \text{ d}^{-1}$ . Using the lower measurement of sulfate reduction, Beggiatoaceae sulfide oxidation could account for only  $\sim 8\%$  of the sulfide turnover. Similar results were reached in studies from Arctic (Jørgensen et al. 2010) and from North Sea sediments (Preisler et al. 2007), where dispersed Beggiatoaceae filaments were likely responsible for oxidizing only a small proportion of the sulfide produced. This accounting suggests that in these sediments either sulfate reduction is overestimated (see Dale et al. 2019 for a discussion of potential overestimation of sulfate reduction rates via the  $^{35}\text{S}$  method), and/or the dominant processes by which sulfide is removed are incompletely quantified. Possible pathways of sulfide removal could include other biological sulfur oxidation pathways, abiotic oxidation by iron or manganese oxides, or sequestration and burial.

### Other benthic sulfur oxidizers

In addition to cable bacteria and Beggiatoaceae, other thiotrophic bacteria may play a quantitatively important role in catalyzing sulfur oxidation (reviewed in Wasmund et al. 2017). In coastal sediments, Campilobacterota (formerly Epsilonproteobacteria) and Gammaproteobacteria may be key players in chemoautotrophic sulfur oxidation, coupling the oxidation of sulfide and/or sulfur compound intermediates with oxygen or nitrate reduction. In the sediments examined here, Campilobacterota, predominantly represented by *Sulfurovum*, constituted an average of 0.12% of all reads (maximum 1.1% at West Station in August 2018; Malkin et al. in submission). These bacteria are capable of sulfide and thiosulfate oxidation (Campbell et al. 2006) and can form biofilms under conditions where high sulfide flux meets oxic or micro-oxic conditions (Meier et al. 2019; Cron et al. 2021). Gammaproteobacteria were abundant in the sediments, constituting 14–30% of reads across samples (Malkin et al. in submission), with Woeseiaceae, a taxon with facultative sulfur oxidation potential (Mußmann et al. 2017) present at 0.5% to 2.9% of the reads. Although the sulfide oxidation potential of Campilobacterota and Gammaproteobacteria may be restricted to sediment zones where sulfide flux intersects with oxygen or nitrate (Jørgensen and Nelson 2004), an analysis of flow-sorted single-cell activity in coastal sediments found that uncultured Gammaproteobacteria were responsible for the vast majority of microbial chemoautotrophy which was dominated by sulfur oxidation (Dyksma et al. 2016). Thus, measuring the relative contributions to sulfide oxidation of Campilobacterota and Gammaproteobacteria, in addition to cable bacteria and Beggiatoaceae, as well as their potential

roles in sulfur compound syntrophic interactions (Vasquez-Cardenas et al. 2015), remains a challenging but exciting area for further research.

## Conclusions

This study investigated the niche partitioning and potential growth constraints of the filamentous thiotrophs, *Candidatus Electrothrix* and Beggiatoaceae, in the sediments of the mesohaline reach of the main stem of Chesapeake Bay. In the seasonally anoxic deep channel, the temporal distribution of cable bacteria suggests a cyclic seasonality—elevated densities of *Ca. E. communis* in winter and spring and only sparse densities in summer and fall—superimposed by hotspots or hot moments of growth of multiple *Candidatus Electrothrix* phylotypes associated with episodic pulses of phytodetritus (i.e., labile organic carbon). At an adjacent depositional shoal site inhabited by deep burrowing infauna, cable bacteria exhibited the same seasonality, but were observed at lower depth-integrated density. Our observations therefore suggest multiple constraints limiting cable bacteria growth, with seasonal anoxia as an important predictor of higher winter and spring biomass accumulation (compared with regions of less severe summer oxygen depletion), and pulses of phytodetritus as an important predictor of their biomass accumulation. Previous work in the Grevelingen reported a similar seasonality of cable bacteria, and furthermore demonstrated that their seasonal abundance may delay bottom water euxinic conditions, due to their impacts on surface sediment iron cycling (Seitaj et al. 2015). By extension, cable bacteria in the main channel of Chesapeake Bay may have system-level impacts on the timing of sulfide efflux from sediments, though this remains to be tested. Our results furthermore demonstrate that the seasonality of cable bacteria may be a general feature of seasonally oxygen depleted marine systems, such as the northern Gulf of Mexico, and that rapid responses to labile organic matter may stimulate different phylotypes or species of cable bacteria.

Beggiatoaceae, by contrast, were typically most abundant at the western shoal site. Their biovolume was positively correlated with potential sediment respiration when free sulfide was not detectable in the sediment surface. Like cable bacteria, Beggiatoaceae were also notably stimulated by the putative hot moment of sulfur cycling at the sediment surface stimulated by a large phytodetritus influx. However, even at their peak biomass accumulation, we estimated these bacteria were unlikely to be capable of oxidizing sulfide at a rate commensurate with its production, implying that other microbial players, abiotic reactions, or formation of sedimentary sulfide (i.e., pyrite or sulfurized organic matter) are likely to be quantitatively important for the removal of sulfide from bioturbated shoal sediments. Together these seasonal and spatial distributions highlight the complexity of the interactions

between these major thiotrophic groups and offer valuable avenues for further enquiry.

## Data availability statement

The data that support the findings of this study are openly available from the Biological and Chemical Oceanography Data Management Office (BCO-DMO; doi: 10.26008/1912/bco-dmo.847974.1; doi: 10.26008/1912/bco-dmo.847923.1; doi: 10.26008/1912/bco-dmo.847949.1; doi: 10.26008/1912/bco-dmo.847846.1). Amplicon sequence libraries are publicly available at the NCBI Sequence Read Archive (Bioproject PRJNA613483; accessions SAMN14407499 to SAMN14407515).

## References

- Ackert, L. 2013. Sergei Vinogradskii and the cycle of life: From the thermodynamics of life to ecological microbiology, 1850–1950. Springer Science & Business Media.
- Aller, R. C., and J. K. Cochran. 2019. The critical role of bioturbation for particle dynamics, priming potential, and organic C remineralization in marine sediments: Local and basin scales. *Front. Earth Sci.* **7**: 157. doi:10.3389/feart.2019.00157
- Aller, R. C., J. Y. Aller, Q. Zhu, C. Heilbrun, I. Klingensmith, and A. Kaushik. 2019. Worm tubes as conduits for the electrogenic microbial grid in marine sediments. *Science Advances* **5**: eaaw3651. doi:10.1126/sciadv.aaw3651
- Barbera, P., A. M. Kozlov, L. Czech, B. Morel, D. Darriba, T. Flouri, and A. Stamatakis. 2019. EPA-ng: Massively parallel evolutionary placement of genetic sequences. *Syst. Biol.* **68**: 365–369. doi:10.1093/sysbio/syy054
- Berger, S. A., and A. Stamatakis. 2011. Aligning short reads to reference alignments and trees. *Bioinformatics* **27**: 2068–2075. doi:10.1093/bioinformatics/btr320
- Bjerg, J. T., and others. 2018. Long-distance electron transport in individual, living cable bacteria. *Proc. Nat. Acad. Sci. USA* **115**: 5786–5791. doi:10.1073/pnas.1800367115
- Booth, J. M., M. Fusi, R. Marasco, T. Mbobo, and D. Daffonchio. 2019. Fiddler crab bioturbation determines consistent changes in bacterial communities across contrasting environmental conditions. *Sci. Rep.* **9**: 3749. doi:10.1038/s41598-019-40315-0
- Braeckman, U., P. Provoost, B. Gribsholt, D. van Gansbeke, J. J. Middelburg, K. Soetaert, M. Vincx, and J. Vanaverbeke. 2010. Role of macrofauna functional traits and density in biogeochemical fluxes and bioturbation. *Mar. Ecol. Prog. Ser.* **399**: 173–186. doi:10.3354/meps08336
- Burdorf, L. D. W., S. Hidalgo-Martinez, P. L. M. Cook, and F. J. R. Meysman. 2016. Long-distance electron transport by cable bacteria in mangrove sediments. *Mar. Ecol. Prog. Ser.* **545**: 1–8. doi:10.3354/meps11635
- Burdorf, L. D. W., S. Y. Malkin, J. T. Bjerg, P. van Rijswijk, F. Criens, A. Tramper, and F. J. R. Meysman. 2018. The effect

- of oxygen availability on long-distance electron transport in marine sediments. *Limnol. Oceanogr.* **63**: 1799–1816. doi:[10.1002/lno.10809](https://doi.org/10.1002/lno.10809)
- Callahan, B. J., P. J. McMurdie, M. J. Rosen, A. W. Han, A. J. A. Johnson, and S. P. Holmes. 2016. DADA2: High-resolution sample inference from Illumina amplicon data. *Nat. Methods* **13**: 581–583. doi:[10.1038/nmeth.3869](https://doi.org/10.1038/nmeth.3869)
- Campbell, B., A. Engel, M. Porter, and K. Takai. 2006. The versatile  $\epsilon$ -proteobacteria: Key players in sulphidic habitats. *Nat. Rev. Microbiol.* **4**: 458–468. doi:[10.1038/nrmicro1414](https://doi.org/10.1038/nrmicro1414)
- Canfield, D. E., R. R. Raiswell, J. T. Westrich, C. M. Reaves, and R. A. Berner. 1986. The use of chromium reduction in the analysis of reduced inorganic sulfur in sediments and shales. *Chem. Geol.* **54**: 149–155. doi:[10.1016/0009-2541\(86\)90078-1](https://doi.org/10.1016/0009-2541(86)90078-1)
- Chanton, J. P., and C. S. Martens. 1985. The effects of heat and stannous chloride addition on the active distillation of acid volatile sulfide from pyrite-rich marine sediment samples. *Biogeochemistry* **1**: 375–382. doi:[10.1007/BF02187379](https://doi.org/10.1007/BF02187379)
- Cron, B., J. L. Macalady, and J. Cosmidis. 2021. Organic stabilization of extracellular elemental sulfur in a sulfurovum-rich biofilm: A new role for extracellular polymeric substances? *Front. Microbiol.* **12**: 720101. doi:[10.3389/fmicb.2021.720101](https://doi.org/10.3389/fmicb.2021.720101)
- Dale, A. W., S. Flury, H. Fossing, P. Regnier, H. Røy, C. Scholze, and B. B. Jørgensen. 2019. Kinetics of organic carbon mineralization and methane formation in marine sediments (Aarhus Bay, Denmark). *Geochim. Cosmochim. Acta* **252**: 159–178. doi:[10.1016/j.gca.2019.02.033](https://doi.org/10.1016/j.gca.2019.02.033)
- Dam, A.-S., I. P. G. Marshall, N. Risgaard-Petersen, L. D. W. Burdorf, and U. Marzocchi. 2021. Effect of salinity on cable bacteria species composition and diversity. *Environ. Microbiol.* **23**: 2605–2616. doi:[10.1111/1462-2920.15484](https://doi.org/10.1111/1462-2920.15484)
- Dunker, R., H. Røy, A. Kamp, and B. B. Jørgensen. 2010. Motility patterns of filamentous sulfur bacteria *Beggiatoa* spp. *FEMS Microbiol. Ecol.* **77**: 176–185. doi:[10.1111/j.1574-6941.2011.01099.x](https://doi.org/10.1111/j.1574-6941.2011.01099.x)
- Dyksma, S., and others. 2016. Ubiquitous Gammaproteobacteria dominate dark carbon fixation in coastal sediments. *ISME J.* **10**: 1939–1953. doi:[10.1038/ISMEJ.2015.257](https://doi.org/10.1038/ISMEJ.2015.257)
- Fenchel, T., and C. Bernard. 1995. Mats of colourless sulphur bacteria. I. Major microbial processes. *Mar. Ecol. Prog. Ser.* **128**: 161–170. doi:[10.3354/meps128161](https://doi.org/10.3354/meps128161)
- Findlay, A. J., A. J. Bennett, T. E. Hanson, and G. W. Luther. 2015. Light-dependent sulfide oxidation in the anoxic zone of the Chesapeake Bay can be explained by small populations of phototrophic bacteria. *Appl. Environ. Microbiol.* **81**: 7560–7569. doi:[10.1128/AEM.02062-15](https://doi.org/10.1128/AEM.02062-15)
- Firsching, F. H. 1961. Precipitation of silver phosphate from homogeneous solution. *Anal. Chem.* **33**: 873–874. doi:[10.1021/ac60175a018](https://doi.org/10.1021/ac60175a018)
- Gomes, M. L., and D. T. Johnston. 2017. Oxygen and sulfur isotopes in sulfate in modern euxinic systems with implications for evaluating the extent of euxinia in ancient oceans. *Geochim. Cosmochim. Acta* **205**: 331–359. doi:[10.1016/j.gca.2017.02.020](https://doi.org/10.1016/j.gca.2017.02.020)
- Graf, G. 1989. Benthic-pelagic coupling in a deep-sea benthic community. *Nature* **341**: 437–439. doi:[10.1038/341437a0](https://doi.org/10.1038/341437a0)
- Harding, L. W., and others. 2015. Climate effects on phytoplankton floral composition in Chesapeake Bay. *Estuar. Coast. Shelf Sci.* **162**: 53–68. doi:[10.1016/j.ecss.2014.12.030](https://doi.org/10.1016/j.ecss.2014.12.030)
- Hermans, M., W. K. Lenstra, S. Hidalgo-Martinez, N. A. G. M. van Helmond, R. Witbaard, F. J. R. Meysman, S. Gonzalez, and C. P. Slomp. 2019. Abundance and biogeochemical impact of cable bacteria in Baltic Sea sediments. *Environ. Sci. Technol.* **53**: 7494–7503. doi:[10.1021/acs.est.9b01665](https://doi.org/10.1021/acs.est.9b01665)
- Jeffrey, G. F., and S. W. Humphrey. 1975. New spectrophotometric equations for determining chlorophylls a, b, c1 and c2 in higher plants, algae and natural phytoplankton. *Biochem. Physiol. Pflanzen.* **167**: 191–194. doi:[10.1016/S0015-3796\(17\)30778-3](https://doi.org/10.1016/S0015-3796(17)30778-3)
- Jiang, L., and M. Xia. 2017. Wind effects on the spring phytoplankton dynamics in the middle reach of the Chesapeake Bay. *Ecol. Model.* **363**: 68–80. doi:[10.1016/j.ecolmodel.2017.08.026](https://doi.org/10.1016/j.ecolmodel.2017.08.026)
- Jochum, L. M., X. Chen, M. A. Lever, A. Loy, B. B. Jørgensen, A. Schramm, and K. U. Kjeldsen. 2017. Depth distribution and assembly of sulfate-reducing microbial communities in marine sediments of Aarhus Bay. *Appl. Environ. Microbiol.* **83**: e01547–e01517. doi:[10.1128/aem.01547-17](https://doi.org/10.1128/aem.01547-17)
- Jørgensen, B. B., and D. C. Nelson. 2004. Sulfide oxidation in marine sediments: Geochemistry meets microbiology, p. 63–81. *In* J. P. Amend, K. Edwards, and T. W. Lyons [eds.], *Sulfur Biogeochemistry—Past and Present*, v. **379**. Special Paper. Geological Society of America.
- Jørgensen, B. B., and A. Boetius. 2007. Feast and famine—microbial life in the deep-sea bed. *Nat. Rev. Microbiol.* **5**: 770–781. doi:[10.1038/nrmicro1745](https://doi.org/10.1038/nrmicro1745)
- Jørgensen, B. B., R. Dunker, S. Grönke, and H. Røy. 2010. Filamentous sulfur bacteria, *Beggiatoaceae* spp., in arctic marine sediments (Svalbard, 79°N). *FEMS Microbiol. Ecol.* **73**: 500–513. doi:[10.1111/j.1574-6941.2010.00918.x](https://doi.org/10.1111/j.1574-6941.2010.00918.x)
- Jørgensen, B. B., A. J. Findlay, and A. Pellerin. 2019. The biogeochemical sulfur cycle of marine sediments. *Front. Microbiol.* **10**: 849. doi:[10.3389/fmicb.2019.00849](https://doi.org/10.3389/fmicb.2019.00849)
- Kallmeyer, J., D. C. Smith, A. J. Spivack, and S. D'Hondt. 2008. New cell extraction procedure applied to deep subsurface sediments. *Limnol. Oceanogr. Methods* **6**: 236–245. doi:[10.4319/lom.2008.6.236](https://doi.org/10.4319/lom.2008.6.236)
- Kemp, W. M., and others. 2005. Eutrophication of Chesapeake Bay: Historical trends and ecological interactions. *Mar. Ecol. Prog. Ser.* **303**: 1–29. doi:[10.3354/meps303001](https://doi.org/10.3354/meps303001)
- Kessler, A. J., and others. 2019. Cable bacteria promote DNRA through iron sulfide dissolution. *Limnol. Oceanogr.* **64**: 1228–1238. doi:[10.1002/lno.11110](https://doi.org/10.1002/lno.11110)

- Kjeldsen, K. U., and others. 2019. On the evolution and physiology of cable bacteria. *Proc. Nat. Acad. Sci. USA* **116**: 19116–19125. doi:[10.1073/pnas.1903514116](https://doi.org/10.1073/pnas.1903514116)
- Kozlov, A. M., D. Darriba, T. Flouri, B. Morel, and A. Stamatakis. 2019. RAXML-NG: A fast, scalable and user-friendly tool for maximum likelihood phylogenetic inference. *Bioinformatics* **35**: 4453–4455. doi:[10.1093/bioinformatics/btz305](https://doi.org/10.1093/bioinformatics/btz305)
- Kristensen, E. 2000. Organic matter diagenesis at the oxic/anoxic interface in coastal marine sediments, with emphasis on the role of burrowing animals. *Hydrobiologia* **426**: 1–24. doi:[10.1023/A:1003980226194](https://doi.org/10.1023/A:1003980226194)
- Kristensen E, and J.E. Kostka. 2005. Macrofaunal burrows and irrigation in marine sediment: Microbiological and biogeochemical interactions. *In*: Kristensen E, Haese RR, Kostka JE (eds). *Interactions between macro- and microorganisms in marine sediments*. American Geophysical Union, p 125–157
- Larsen, S., L. P. Nielsen, and A. Schramm. 2014. Cable bacteria associated with long-distance electron transport in New England salt marsh sediment. *Environ. Microbiol. Rep.* **7**: 175–179. doi:[10.1111/1758-2229.12216](https://doi.org/10.1111/1758-2229.12216)
- Lehto, N., R. N. Glud, and G. á Norði, H. Zhang, and W. Davison. 2014. Anoxic microniches in marine sediments induced by aggregate settlement: Biogeochemical dynamics and implications. *Biogeochem.* **119**: 307–327. doi:[10.1007/s10533-014-9967-0](https://doi.org/10.1007/s10533-014-9967-0)
- Lever, M. A., A. Torti, P. Eickenbusch, A. B. Michaud, T. Šantl-Temkiv, and B. B. Jørgensen. 2015. A modular method for the extraction of DNA and RNA, and the separation of DNA pools from diverse environmental sample types. *Front. Microbiol.* **6**: 476. doi:[10.3389/fmicb.2015.00476](https://doi.org/10.3389/fmicb.2015.00476)
- Love, M. I., W. Huber, and S. Anders. 2014. Moderated estimation of fold change and dispersion for RNA-seq data with DESeq2. *Genome Biol.* **15**: 550. doi:[10.1186/s13059-014-0550-8](https://doi.org/10.1186/s13059-014-0550-8)
- Lunau, M., A. Lemke, K. Walther, W. Martens-Habbena, and M. Simon. 2005. An improved method for counting bacteria from sediments and turbid environments by epifluorescence microscopy. *Environ. Microbiol.* **7**: 961–968. doi:[10.1111/j.1462-2920.2005.00767.x](https://doi.org/10.1111/j.1462-2920.2005.00767.x)
- Malkin, S. Y., D. Seitaj, D. Vasquez-Cardenas, E.-M. Zetsche, S. Hidalgo-Martinez, H. T. S. Boschker, and F. J. R. Meysman. 2015. Natural occurrence of microbial sulphur oxidation by long-distance electron transport in the seafloor. *ISME J.* **8**: 1843–1854. doi:[10.1038/ismej.2014.41](https://doi.org/10.1038/ismej.2014.41)
- Malkin, S. Y., and others. 2017. Electrogenic sulphide oxidation by cable bacteria in bivalve reef sediments. *Front. Mar. Sci.* **4**: 28. doi:[10.3389/fmars.2017.00028](https://doi.org/10.3389/fmars.2017.00028)
- Martin, B. C., J. Bougoure, M. H. Ryan, W. W. Bennett, T. D. Colmer, N. K. Joyce, Y. S. Olsen, and G. A. Kendrick. 2019. Oxygen loss from seagrass roots coincides with colonisation of sulphide-oxidising cable bacteria and reduces sulphide stress. *ISME J.* **13**: 707–719. doi:[10.1038/s41396-018-0308-5](https://doi.org/10.1038/s41396-018-0308-5)
- Marvin-DiPasquale, M. C., W. R. Boynton, and D. G. Capone. 2003. Benthic sulfate reduction along the Chesapeake Bay central channel. II. Temporal controls. *Mar. Ecol. Prog. Ser.* **260**: 55–70. doi:[10.3354/meps260055](https://doi.org/10.3354/meps260055)
- Marzocchi, U., and others. 2014. Electric coupling between distant nitrate reduction and sulfide oxidation in marine sediment. *ISME J.* **8**: 1682–1690. doi:[10.1038/ismej.2014.19](https://doi.org/10.1038/ismej.2014.19)
- Marzocchi, U., S. Bonaglia, S. van de Velde, P. O. J. Hall, A. Schramm, N. Risgaard-Petersen, and F. J. R. Meysman. 2018. Transient bottom water oxygenation creates a niche for cable bacteria in long-term anoxic sediments of the Eastern Gotland Basin. *Environ. Microbiol.* **20**: 3031–3041. doi:[10.1111/1462-2920.14349](https://doi.org/10.1111/1462-2920.14349)
- Marzocchi, U., C. Thorup, C., A.-S. Dam, A. Schramm, and N. Risgaard-Petersen. 2022. Dissimilatory nitrate reduction by a freshwater cable bacterium. *ISME J.* **16**: 50–57. doi:[10.1038/s41396-021-01048-z](https://doi.org/10.1038/s41396-021-01048-z)
- McMurdie, P. J., and S. Holmes. 2013. phyloseq: An R package for reproducible interactive analysis and graphics of microbiome census data. *PLoS One* **8**: e61217. doi:[10.1371/journal.pone.0061217](https://doi.org/10.1371/journal.pone.0061217)
- Meier, D. V., and others. 2019. Microbial metal-sulfide oxidation in inactive hydrothermal vent chimneys suggested by metagenomic and metaproteomic analyses. *Environ. Microbiol.* **21**: 682–701. doi:[10.1111/1462-2920.14514](https://doi.org/10.1111/1462-2920.14514)
- Meysman, F. J. R., N. Risgaard-Petersen, S. Y. Malkin, and L. P. Nielsen. 2015. The geochemical fingerprint of microbial long-distance electron transport in the seafloor. *Geochem. Cos. Acta* **152**: 122–142. doi:[10.1016/j.gca.2014.12.014](https://doi.org/10.1016/j.gca.2014.12.014)
- Moeslund, L., B. Thamdrup, and B. B. Jørgensen. 1994. Sulfur and iron cycling in a coastal sediment: Radiotracer studies and seasonal dynamics. *Biogeochemistry* **27**: 129–152. doi:[10.1007/BF00002815](https://doi.org/10.1007/BF00002815)
- Murali, A., A. Bhargava, and E. S. Wright. 2018. IDTAXA: A novel approach for accurate taxonomic classification of microbiome sequences. *Microbiome* **6**: 140. doi:[10.1186/s40168-018-0521-5](https://doi.org/10.1186/s40168-018-0521-5)
- Mußmann, M., H. N. Schulz, B. Strotmann, T. Kjær, L. P. Nielsen, R. A. Rössello-Mora, R. I. Amann, and B. B. Jørgensen. 2003. Phylogeny and distribution of nitrate-storing Beggiatoaceae spp. in coastal marine sediments. *Environ. Microbiol.* **5**: 523–533. doi:[10.1046/j.1462-2920.2003.00440.x](https://doi.org/10.1046/j.1462-2920.2003.00440.x)
- Mußmann, M., and others. 2007. Insights into the genome of large sulfur bacteria revealed by analysis of single filaments. *PLoS Biol.* **5**: e230. doi:[10.1371/journal.pbio.0050230](https://doi.org/10.1371/journal.pbio.0050230)
- Mußmann, M., P. Pjevac, K. Krüger, and S. Dykstra. 2017. Genomic repertoire of the Woeseiaceae/JTB255, cosmopolitan and abundant core members of microbial communities in marine sediments. *ISME J.* **11**: 1276–1281. doi:[10.1038/ismej.2016.185](https://doi.org/10.1038/ismej.2016.185)
- Nielsen, L. P., and N. Risgaard-Petersen. 2015. Rethinking sediment biogeochemistry after the discovery of electric

- currents. *Ann. Rev. Mar. Sci.* **7**: 21.1–21.18. doi:[10.1146/annurev-marine-010814-015708](https://doi.org/10.1146/annurev-marine-010814-015708)
- Nielsen, L. P., N. Risgaard-Petersen, H. Fossing, P. B. Christensen, and M. Sayama. 2010. Electric currents couple spatially separated biogeochemical processes in marine sediment. *Nature* **463**: 1071–1074. doi:[10.1038/nature08790](https://doi.org/10.1038/nature08790)
- Oksanen, J., and others. 2019. vegan: Community Ecology Package. R package version 2.5-6.
- Papasprou, S., T. Gregersen, E. Kristensen, B. Christensen, and R. P. Cox. 2006. Microbial reaction rates and bacterial communities in sediment surrounding burrows of two nereidid polychaetes (*Nereis diversicolor* and *N. virens*). *Mar. Biol.* **148**: 541–550. doi:[10.1007/s00227-005-0105-3](https://doi.org/10.1007/s00227-005-0105-3)
- Parada, A. E., D. M. Needham, and J. A. Fuhrman. 2015. Every base matters: Assessing small subunit rRNA primers for marine microbiomes with mock communities, time series and global field samples. *Environ. Microbiol.* **18**: 1403–1414. doi:[10.1111/1462-2920.13023](https://doi.org/10.1111/1462-2920.13023)
- Pernthaler, J., F. O. Glockner, W. Schonhuber, and R. Amann. 2001. Fluorescence in situ hybridization (FISH) with rRNA-targeted oligonucleotide probes. *Method. Microbiol.* **30**: 207–226. doi:[10.1016/S0580-9517\(01\)30046-6](https://doi.org/10.1016/S0580-9517(01)30046-6)
- Pfeffer, C., and others. 2012. Filamentous bacteria transport electrons over centimeter distances. *Nature* **491**: 218–221. doi:[10.1038/nature11586](https://doi.org/10.1038/nature11586)
- Preisler, A., D. de Beer, A. Lichtschlag, G. Lavik, A. Boetius, and B. B. Jørgensen. 2007. Biological and chemical sulfide oxidation in a Beggiatoaceae inhabited marine sediment. *ISME J.* **1**: 341–353. doi:[10.1038/ismej.2007.50](https://doi.org/10.1038/ismej.2007.50)
- Pruesse, E., C. Quast, K. Knittel, B. M. Fuchs, W. Ludwig, J. Peplies, and F. O. Glöckner. 2007. SILVA: A comprehensive online resource for quality checked and aligned ribosomal RNA. *Nucleic Acids Res.* **35**: 7188–7196. doi:[10.1093/nar/gkm864](https://doi.org/10.1093/nar/gkm864)
- Rao, A. M. F., S. Y. Malkin, F. Montserrat, and F. J. R. Meysman. 2014. Enhanced alkalinity production in intertidal sands from the Oosterschelde (The Netherlands) induced by the lugworm *Arenicola marina*. *Estuar. Coast. Sea Res.* **148**: 36–47. doi:[10.1016/j.ecss.2014.06.006](https://doi.org/10.1016/j.ecss.2014.06.006)
- Rao, A. M. F., S. Y. Malkin, S. Hidalgo-Martinez, and F. J. R. Meysman. 2016. The impact of electrogenic sulfide oxidation on elemental cycling and solute fluxes in coastal sediment. *Geochim. Cosmochim. Acta* **172**: 265–286. doi:[10.1016/j.gca.2015.09.014](https://doi.org/10.1016/j.gca.2015.09.014)
- Risgaard-Petersen, N., A. Revil, P. Meister, and L. P. Nielsen. 2012. Sulphur, iron and calcium cycling associated with natural electric currents running through marine sediments. *Geochim. Cosmochim. Acta* **92**: 1–13. doi:[10.1016/j.gca.2012.05.036](https://doi.org/10.1016/j.gca.2012.05.036)
- Risgaard-Petersen, N., L. R. Damgaard, A. Revil, and L. P. Nielsen. 2014. Mapping electron sources and sinks in a marine biogeochemical battery. *J. Geophys. Res. Biogeophys.* **119**: 1475–1486. doi:[10.1002/2014JG002673](https://doi.org/10.1002/2014JG002673)
- Roden, E. E., and J. H. Tuttle. 1993. Inorganic sulfur cycling in mid and lower Chesapeake Bay sediments. *Mar. Ecol. Prog. Ser.* **93**: 101–118. doi:[10.1007/BF00002706](https://doi.org/10.1007/BF00002706)
- Rodil, I. F., P. Lucena-Moya, T. Tamelander, J. Norkko, and A. Norkko. 2020. Seasonal variability in benthic–pelagic coupling: Quantifying organic matter inputs to the seafloor and benthic macrofauna using a multi-marker approach. *Front. Mar. Sci.* **7**: 404. doi:[10.3389/fmars.2020.00404](https://doi.org/10.3389/fmars.2020.00404)
- Salman, V., R. Amann, D. A. Shub, and H. N. Schulz-Vogt. 2012. Multiple self-splicing introns in the 16S rRNA genes of giant sulfur bacteria. *Proc. Nat. Acad. Sci. USA* **109**: 4203–4208. doi:[10.1073/pnas.1120192109](https://doi.org/10.1073/pnas.1120192109)
- Sandfeld, T., U. Marzocchi, C. Petro, A. Schramm, and N. Risgaard-Petersen. 2020. Electrogenic sulfide oxidation mediated by cable bacteria stimulates sulfate reduction in freshwater sediments. *ISME J.* **14**: 1233–1246. doi:[10.1038/s41396-020-0607-5](https://doi.org/10.1038/s41396-020-0607-5)
- Sayama, M., N. Risgaard-Petersen, L. P. Nielsen, H. Fossing, and P. B. Christensen. 2005. Impact of bacterial NO<sub>3</sub><sup>-</sup> transport on sediment biogeochemistry. *Appl. Environ. Microbiol.* **71**: 7575–7577. doi:[10.1128/AEM.71.11.7575-7577.2005](https://doi.org/10.1128/AEM.71.11.7575-7577.2005)
- Schauer, R., N. Risgaard-Petersen, K. U. Kjeldsen, J. T. Bjerg, B. B. Jørgensen, A. Schramm, and L. P. Nielsen. 2014. Succession of cable bacteria and electric currents in marine sediment. *ISME J.* **8**: 1314–1322. doi:[10.1038/ismej.2013.239](https://doi.org/10.1038/ismej.2013.239)
- Scholz, V. V., and others. 2021. Cable bacteria at oxygen-releasing roots of aquatic plants: A widespread and diverse plant–microbe association. *New Phytol.* **232**: 2138–2151. doi:[10.1111/nph.17415](https://doi.org/10.1111/nph.17415)
- Schwedt, A., A.-C. Kreutzmann, L. Polerecky, and H. N. Schulz-Vogt. 2012. Sulfur respiration in a marine chemolithoautotrophic *Beggiatoa* strain. *Front. Microbiol.* **2**: 276. doi:[10.3389/fmicb.2011.00276](https://doi.org/10.3389/fmicb.2011.00276)
- Seitaj, D., R. Schauer, F. Sulu-Gambari, S. Hidalgo-Martinez, S. Y. Malkin, L. D. Burdorf, C. P. Slomp, and F. J. R. Meysman. 2015. Cable bacteria generate a firewater against euxinia in seasonally hypoxic basins. *Proc. Nat. Acad. Sci. USA* **112**: 13278–13283. doi:[10.1073/pnas.1510152112](https://doi.org/10.1073/pnas.1510152112)
- Soetaert, K., T. Petzoldt, F. Meysman, and L. Meire. 2020. *marelac*: Tools for Aquatic Sciences. R package v 2.1.10.
- Sturdivant, S. K., R. J. Díaz, and G. R. Cutter. 2012. Bioturbation in a declining oxygen environment, *in situ* observations from wormcam. *PLoS One* **7**: e34539. doi:[10.1371/journal.pone.0034539](https://doi.org/10.1371/journal.pone.0034539)
- Sulu-Gambari, F., D. Seitaj, F. J. R. Meysman, R. Schauer, L. Polerecky, and C. P. Slomp. 2015. Cable bacteria control iron-phosphorus dynamics in sediments of a coastal hypoxic basin. *Environ. Sci. Technol.* **50**: 1227–1233. doi:[10.1021/acs.est.5b04369](https://doi.org/10.1021/acs.est.5b04369)
- Sulu-Gambari, F., D. Seitaj, T. Behrends, D. Banerjee, F. J. R. Meysman, and C. P. Slomp. 2016. Impact of cable bacteria on sedimentary iron and manganese dynamics in a seasonally-hypoxic marine basin. *Geochim. Cosmochim. Acta* **192**: 49–69. doi:[10.1016/j.gca.2016.07.028](https://doi.org/10.1016/j.gca.2016.07.028)

- Teske, A., and V. Salman. 2014. The family Beggiatoaceae, p. 93–134. In E. Rosenberg, D. L. EF, S. Lory, E. Stackebrandt, and F. Thompson [eds.], *The prokaryotes: Gammaproteobacteria*. Springer. doi:10.1007/978-3-642-38922-1\_290
- Thamdrup, B., H. H. Fossing, and B. B. Jørgensen. 1994. Manganese, iron, and sulfur cycling in a coastal marine sediment, Aarhus Bay, Denmark. *Geochim. Cosmochim. Acta* **58**: 5115–5129. doi:10.1016/0016-7037(94)90298-4
- Trojan, D., L. Schreiber, J. T. Bjerg, A. Bøggild, T. Yang, J. U. Kjeldsen, and A. Schramm. 2016. A taxonomic framework for cable bacteria and proposal of the candidate genera *Electrothrix* and *Electronema*. *Syst. Appl. Microbiol.* **39**: 297–306. doi:10.1016/j.syapm.2016.05.006
- van de Velde, S., L. Lesven, L. D. W. Burdorf, S. Hidalgo-Martinez, J. S. Geelhoed, P. van Rijswijk, Y. Gao, and F. J. R. Meysman. 2016. The impact of electrogenic sulfur oxidation on the biogeochemistry of coastal sediments: A field study. *Geochim. Cosmochim. Acta* **194**: 211–232. doi:10.1016/j.gca.2016.08.038
- van de Velde, S., I. Callebaut, Y. Gao, and F. J. R. Meysman. 2017. Impact of electrogenic sulfur oxidation on trace metal cycling in a coastal sediment. *Chem. Geol.* **452**: 9–23. doi:10.1016/j.chemgeo.2017.01.028
- Vasquez-Cardenas, D., and others. 2015. Microbial carbon metabolism associated with electrogenic sulphur oxidation in coastal sediments. *ISME J.* **9**: 1966–1978. doi:10.1038/ismej.2015.10
- Wasmund, K., M. Mußmann, and A. Loy. 2017. The life sulfuric: Microbial ecology of sulfur cycling in marine sediments. *Enviro. Micro. Rep.* **9**: 323–344. doi:10.1111/1758-2229.12538
- Wright, E. S. 2015. DECIPHER: Harnessing local sequence context to improve protein multiple sequence alignment. *BMC Bioinf* **16**: 322. doi:10.1186/s12859-015-0749-z
- Yu, G. D., H. Smith, Y. Zhu, T. T.-Y. Guan, and Lam. 2017. *ggtree*: An R package for visualization and annotation of phylogenetic trees with their covariates and other associated data. *Mol. Ecol. Evol.* **8**: 28–36. doi:10.1111/2041-210X.12628
- Zimmerman, A. R., and E. A. Canuel. 2002. Sediment geochemical records of eutrophication in the mesohaline Chesapeake Bay. *Limnol. Oceanogr.* **47**: 1084–1093. doi:10.4319/lo.2002.47.4.1084

### Acknowledgments

The authors gratefully acknowledge Andy McCarthy and Emily Wolcott for assistance in the field, Sabeena Nazar for DNA amplification and sequencing, and Clara Fuchsman for assistance with phylogenetic tree construction. This work was funded by UMCES new faculty start-up funds (SM), National Science Foundation (OCE-1756877; SM), UMCES Presidential Fellowship (PL), HPL fellowship (CK), and American Chemical Society Petroleum Research Funding (MG).

### Conflict of Interest

The authors have no competing interests to declare that are relevant to the content of this article.

Submitted 21 September 2021

Revised 30 January 2022

Accepted 27 March 2022

Associate editor: Osvaldo Ulloa